

NASA TECHNICAL NOTE



NASA TN D-3923

NASA TN D-3923

N 67 - 25040

FACILITY FORM 602	_____ (ACCESSION NUMBER) 48	_____ (THRU)
	_____ (PAGES)	_____ (CODE) 1
	_____ (NASA CR OR TMX OR AD NUMBER)	_____ (CATEGORY) 17

FIBERING OF OXIDES IN REFRACTORY-METAL MATRICES

by Robert W. Jech, John W. Weeton, and Robert A. Signorelli

Lewis Research Center

Cleveland, Ohio

FIBERING OF OXIDES IN REFRACTORY-METAL MATRICES

By Robert W. Jech, John W. Weeton, and Robert A. Signorelli

Lewis Research Center
Cleveland, Ohio

NATIONAL AERONAUTICS AND SPACE ADMINISTRATION

For sale by the Clearinghouse for Federal Scientific and Technical Information
Springfield, Virginia 22151 - CFSTI price \$3.00

FIBERING OF OXIDES IN REFRACTORY-METAL MATRICES

by Robert W. Jech, John W. Weeton, and Robert A. Signorelli

Lewis Research Center

SUMMARY

Combinations of oxides and refractory metals were investigated in order to determine the conditions under which oxides could be made to elongate during mechanical working to form fibers and thereby provide reinforcement for refractory metals. Metallographic examination was used to classify the microstructure of the composites, and tensile and stress-rupture tests were employed to determine mechanical properties. Composites containing fibered oxides exhibited mechanical properties markedly superior to the additive-free base materials, while composites in which fiberling of the oxide did not occur showed little or no improvement in these mechanical properties.

The correlation between the length-diameter ratio of the fibered oxides and the elevated-temperature tensile strength of the composites could not be made, although some indication of a correlation between the length-diameter ratio and the stress-rupture properties was indicated. The actual fiberling of the oxides was related to the crystal structure of the oxide, the extrusion temperature, and the extrusion ratio at which reduction was accomplished.

INTRODUCTION

Candidate metals for use in many high-temperature applications are limited to the refractory metals: tungsten, molybdenum, tantalum, and columbium. These metals are characterized by their high melting point ($>4000^{\circ}\text{F}$), and considerable work has been directed toward further improvement of their high-temperature strength. The use of alloying elements has improved the high-temperature properties of these materials; however, such additions may not yield the longtime stability desired.

Metal oxides may also be considered as alternate candidate materials for high-temperature applications. Many are chemically stable, highly refractory, and, in addition, of low density. They are characterized by resistance to creep at elevated

temperatures, and they show little change in tensile strength over a wide range of temperatures. Most oxides are quite brittle, particularly in massive form, and it is only in whisker form that they have exhibited their very high tensile strength.

Both refractory metals and oxide fibers exhibit some of the desired properties for high-temperature applications, but neither material alone has the combination of strength and ductility desired. One possible approach to achieving this combination would be to combine the oxide and metal in a fiber-reinforced composite similar to that in which a metal fiber is used to reinforce a metal matrix (ref. 1). In such fiber-reinforced composites, it may be possible to obtain the maximum benefit from each component while minimizing the undesirable properties of each. Two examples of such oxide-reinforced-metal composites are aluminum oxide whiskers in silver (ref. 2) and silica fibers in aluminum (ref. 3). In these investigations, as well as in others, fibers or whiskers were produced separately and then incorporated into the matrix to form the composite. Such a process has certain inherent disadvantages. Oxide fibers and whiskers are subject to a degradation in mechanical properties due to handling. The atmosphere in which they are produced and stored can also have a profound effect upon their mechanical properties (ref. 4). Solutions to the problem of fiber damage have met with some success. Other investigators have used a protective coating that is applied to the fiber immediately after it is produced (ref. 5); this application introduces the necessity for eliminating the coating prior to incorporating the fiber into a composite or for utilizing the coating as an alloying or bonding agent.

Work at the NASA Lewis Research Center (ref. 6) has resulted in the development of composites in which the oxide or refractory hard metal fibers were produced within a tungsten matrix during high-temperature working. A considerable increase in the stress-rupture life of these composites was obtained; however, determination of the actual contribution of the fiber as reinforcement was not made.

Formation of oxide fibers within the matrix eliminates handling the fibers. Because the oxide does not exist as a fiber until after it has been incorporated into the matrix, there is no need for a protective coating. Since new surfaces are created at the matrix-fiber interface, the bond between the fiber and the matrix should be enhanced.

The objectives of this investigation were to determine whether oxide particles, which in some cases had a modulus of elasticity greater than that of the metal matrix, could be fibered when mechanically deformed in a ductile metal matrix at high temperature; to determine the effect of processing parameters on the degree of fiberizing achieved; and to determine the effect of the incorporated oxide fibers on the ultimate tensile strength and the stress-rupture strength of columbium- and tantalum-based composites at room and elevated temperatures.

Most of the investigation was carried out by using unalloyed columbium or tantalum as the matrix material and magnesium oxide, thorium oxide, aluminum oxide, or

zirconium oxide as the oxide. Composites were prepared by powder-metallurgy methods and extruded or rolled at an elevated temperature. Composites were examined for microstructure and hardness and were tested in tension at room temperature and at 1100°, 2200°, 2500°, 2750°, and 3000° F. In addition, stress-rupture tests of the composites were conducted in vacuum at 2200° and 2500° F for times up to 1000 hours.

MATERIALS, APPARATUS, AND PROCEDURE

Materials Selection

Columbium and tantalum were selected as the primary matrix materials for this investigation because of their high melting point, moderate modulus of elasticity, and good ductility at room and elevated temperature. Selection of the oxides was based upon their melting point, thermodynamic stability in the presence of columbium or tantalum, and modulus of elasticity.

Melting point was significant in making the materials selection. In the case of the matrix, it was important to have a material that melted at a temperature above that at which mechanical working was to be carried out. Mechanical deformation of the oxide from equiaxed particles into elongated fibers imposed the requirement that the softening temperature of the oxide be below the melting point of the matrix. Since few data on the softening temperature of oxides were available, it was necessary to use melting point data.

Modulus of elasticity was also used as one of the criteria for materials selection. It has been shown that, except in certain special cases, the most efficient reinforcing fibers were those having a modulus greater than or equal to that of the matrix (ref. 1).

The data for the melting point and the modulus of elasticity were plotted as shown in figure 1 (data from ref. 7). By noting the position of the various oxides as they related to the melting point and modulus of the matrix, a first selection of candidate oxides was made. The combinations magnesium oxide - tantalum and aluminum oxide - columbium were selected.

Several other combinations of materials were also used in this investigation, although they did not necessarily appear promising on the basis of modulus of elasticity or melting point. These other materials were used because previous investigators had reported (ref. 8) that the softening temperatures of some oxides could be as low as 50 percent of the melting temperature; for this reason, oxides having melting points higher than that of the metal matrix were included. A complete list of the combinations tested is given in table I.

After the combinations of materials were selected, they were checked for com-

patibility. This check was made by comparing the relative free energies of formation of the oxide and the possible matrix oxides at the highest temperature to be encountered by the combination during either processing or testing. Data for these comparisons were obtained from standard tables (ref. 9). When possible, the combinations were also checked against the result of actual compatibility studies, as reported in references 10 and 11.

Composite Preparation

Extrusion billets of the various oxide-metal combinations listed in table I were prepared by using the starting materials listed in table II. The combinations of ceramic and metal powders were dry blended in a twin shell V-blender and hydrostatically cold pressed at 50 000 pounds per square inch. Billets of the matrix material without oxide additives were included for use as control or base-line data.

Sintering was done in a resistance-heated vacuum furnace, at the sintering temperatures and times listed in table I. A pressure of 10^{-4} torr or less was maintained during heating. Once the desired temperature was reached, a vacuum of 5×10^{-5} torr was usual during the remainder of the run. After being held at temperature for 4 hours, the billets were furnace cooled to room temperature.

The sintered billets were machined to their final dimensions and canned in heavy-walled (1/4 in.) powder-metallurgy molybdenum extrusion cans. In order to minimize contamination, all billet and can machining was accomplished without the use of a lubricant. A sketch of the extrusion can is shown in figure 2(a), and a photograph of a canned billet ready for extrusion is presented in figure 2(b). The plug at the butt end of the can was welded in place in an evacuated chamber (10^{-5} torr) by using an electron-beam welder. In this way, a tight, clean weld was obtained.

A 1020-ton hydraulic extrusion press, as described in reference 12, was used to extrude the sintered billets. An induction heating source was employed to heat the billet in a protective atmosphere of hydrogen. After the billet was brought to the desired temperature (given in table I), it was held for 10 to 15 minutes and extruded. Total time from the induction heater to the completed extrusion was from 4.5 to 7 seconds.

In order to determine how effective extrusion was in producing a fibered oxide structure, the microstructure of each composite was examined in specimens from the nose, middle, and tail sections of the extrusion. This examination was made as soon as possible after extrusion so that adjustments in extrusion temperature and/or extrusion ratio could be made for succeeding composites.

Tensile and stress-rupture specimens were prepared from the remaining portions of the extrusion. In addition, density measurements by the water displacement method

were made on each specimen.

The data relating the stiffness of the matrix to oxide fibering were obtained by using hot rolling as the primary fabrication technique. These specimens were prepared by cold-pressing dry-blended 1.55-micron zirconium oxide powder and columbium, tungsten, or tantalum into 1/4- by 1/4- by 4-inch bars at 50 000 pounds per square inch. The columbium and tantalum bars were sintered for 4 hours at 3700° F in vacuum, and the tungsten bars were sintered for 4 hours at 4000° F. The composites were hot rolled at either 3500° or 3800° F with flat rolls. An induction heating source was located immediately adjacent to the rolls in order to minimize heat loss during transfer. The first pass through the rolls produced a 25-percent reduction in area of the sintered compacts. Subsequent passes resulted in total reductions in area of 50, 75, and 90 percent, respectively. After each pass, samples were taken for metallographic examination and measurement of fiber length-diameter ratio.

Composite Examination and Testing

The microstructure of the longitudinal and transverse sections of each hot-worked sample was examined. Photographs of the longitudinal sections were taken, and three random bands located adjacent to the extrusion centerline were marked out on the photographs. The length and diameter of each fiber in the bands were measured. From these measurements, the length-diameter ratio (L/D) and the area of each fiber were calculated. The total area occupied by all the fibers of a specific L/D range was calculated as was the total area for all the fibers. The data for each sample were then plotted as shown in the example in figure 3. The L/D at 50 percent was used as an approximate measure of fibering in the composites. Fifty percent of all the area occupied by fibers was occupied by those fibers having an L/D of 6.5 or greater (fig. 3).

Tensile tests were conducted by using a crosshead speed of 0.10 inch per minute. All tests, with the exception of the room-temperature tests, were performed in a vacuum chamber at a pressure of at least 10^{-5} torr. Elevated-temperature tensile tests were run at 1100°, 2200°, 2500°, 2750°, and 3000° F. Details of this testing apparatus are given in reference 13, and a sketch of the specimen used is shown in figure 4.

Stress-rupture tests were conducted in high-temperature stress-rupture machines of NASA design (ref. 14). The specimens were protected by testing in a vacuum chamber at a pressure of 10^{-5} torr. A liquid-nitrogen-cooled baffle was used to prevent backstreaming of diffusion-pump oil. An estimate of the creep rate was obtained by measuring specimen elongation with a dial indicator connected to the loading train.

Samples of a typical oxide - fiber-metal composite, as well as of additive-free columbium, were tested for hardness in the as-extruded and extruded, heat-treated

conditions. The heat treatment was executed in a vacuum of 10^{-5} torr for 100 hours at 2200° F. The specimens were sectioned, polished, and etched to reveal the structure in the plane parallel to the extrusion direction. Hardness measurements were made on the matrix and oxide fibers in the composites and on additive-free columbium by using a Knoop indenter and a 25-gram load.

RESULTS

Effect of Extrusion on Fiberling

Microstructures of 17 and 20 volume percent zirconium oxide - columbium composites are shown in figure 5. Figure 5(a) shows the structure of a cold-pressed and sintered billet (90 percent of theoretical density) prior to extrusion; figures 5(b), (d), and (f) show unetched, longitudinal sections of composites extruded at 3500° F at nominal extrusion ratios of 20:1 ($L/D = 6.5$), 24:1 ($L/D = 8.4$), and 32:1 ($L/D = 9.0$), respectively. Figure 5(c) shows the same view of an extrusion carried out at 3800° F at a ratio of 20:1 ($L/D = 11.1$). A transverse section that was considered typical of all the extruded composites is shown in figure 5(e). From an examination of the longitudinal sections, it is immediately apparent that the degree of elongation or fiberling of the oxide, as would be expected, is greater at the higher extrusion ratios. A comparison of figures 5(b) and (c) indicated that extrusion at a higher temperature (3800° F as compared with 3500° F) and at a constant extrusion ratio results in an improvement in fiberling ($L/D = 11.1$ as compared with $L/D = 6.5$).

At this point, some comment regarding fiberling as it relates to sample position within the extrusion is in order. Figure 6 shows longitudinal sections taken from the nose, middle, and tail sections of an extrusion containing 20 volume percent zirconium oxide in columbium made at 3500° F and an extrusion ratio of 20:1. Some differences in the amount of fiberling at various positions along the length of the composite may be seen. The L/D of the fibers at the nose of the extruded composite was 4.5; at the middle section of the composite, 6.5; at the tail section of the composite, 4.6. Portions of the composite that exhibited the nose and tail type structure were confined to about 10 percent of the total length of the extrusion, and these portions were not used for test specimens.

Examination of the composite microstructure from the center of the rod to the outer edge indicated that the degree of fiberling varied from the center of the extrusion radially outward to the core-cladding interface, with the greatest degree of fiberling taking place near the interface. Since this outer layer was removed during machining of the test specimens, all photomicrographs and estimations of fiberling were based upon the

structure observed nearest the centerline of the extruded core.

Figure 7 shows the microstructure of a 17-volume-percent zirconium oxide - columbium composite in the etched condition and also the microstructure of an additive-free columbium control sample. Both pictures show longitudinal sections of extrusions that were made at a ratio of 20:1 and a temperature of 3500⁰ F. Both composites are in the as-extruded condition. The difference in grain size between the two is immediately apparent. The microstructure of the composite is that of oxide fibers in a very fine-grained columbium matrix, while the additive-free columbium shows a structure of very coarse grains containing impurity particles, presumably columbium oxide.

Composites composed of 20 volume percent thorium oxide in columbium and additive-free columbium control specimens processed in the same way are shown in figure 8. Those thorium oxide - columbium composites shown in figures 8(b) and (c) were both extruded at a ratio of 16:1 and temperatures of 3200⁰ and 3500⁰ F, respectively. Their structure, with respect to fibering, is almost the same (L/D = 1.6 and 1.1). The composite shown in figure 8(d) was extruded at 3200⁰ F but at a ratio of 32:1; its fibers are considerably longer and have an L/D of 9.0.

The microstructure of 20-volume-percent magnesium oxide - tantalum composites is shown in figure 9. The microstructure of a billet in the as-sintered condition is presented in figure 9(a). Some of the areas contain rather large magnesium oxide agglomerates, and it can be seen from the succeeding photographs that these agglomerates are partially broken up or deformed during the extrusion operation. Figures 9(c), (d), and (e) show longitudinal sections of magnesium oxide - tantalum composites that were extruded at a ratio of 16:1 and 3200⁰ F (L/D = 6.0), 16:1 and 3500⁰ F (L/D = 10.4), and 24:1 and 3500⁰ F (L/D = 5.7), respectively. While some fibering had taken place in all the magnesium oxide - tantalum composites, the extent of fibering was not as great as that observed in the composites of zirconium oxide and columbium or thorium oxide and columbium.

Composites containing aluminum oxide in columbium, silica in tungsten, alumina silicate in tungsten, and glass in aluminum were also extruded. These were not successfully fibered. Figure 10(a) shows a 20-volume-percent aluminum oxide - columbium composite before extrusion, while figure 10(b) shows a longitudinal section after extrusion at a ratio of 8:1 and 3000⁰ F.

Figures 10(c) and (d) present longitudinal sections of silica-tungsten composites that were extruded at a ratio of 8:1 and temperatures of 3000⁰ and 3200⁰ F. No fibering is evident.

Figure 10(e) shows a longitudinal section of a composite containing glass dispersed in a matrix of aluminum. The extrusion was done at a ratio of 16:1 and a temperature of 1100⁰ F. It is evident that the glass did not deform during extrusion.

Effect of Rolling on Fiberling

A series of composites was fabricated by utilizing hot rolling as the primary method of densification and oxide fiberling. Composites containing zirconium oxide in columbium, tantalum, and tungsten were used.

Photomicrographs of sections of as-sintered and hot-rolled composites containing zirconium oxide in columbium, tantalum, and tungsten are shown in figures 11, 12, and 13, respectively. Examination of the photomicrographs indicates that densification occurred during the early stages of hot rolling and that little fiberling of the oxide took place. As the amount of hot-work increased, the oxide particles became oriented parallel to the direction of rolling, and fiberling began.

Length-Diameter Ratio

The results of L/D measurements are presented in table III, and figure 14 shows the variation of the L/D of oxide fibers produced by extrusion as a function of the extrusion temperature. In the range of extrusion temperatures utilized, the effect of increased temperature on fiber formation is most pronounced in the magnesium oxide - tantalum composites. The fiberling tendency is less for fibers in the zirconium oxide - columbium composites, particularly at the lower temperatures, although at the higher temperature (3800°F) fiberling is enhanced. Composites containing thorium oxide in columbium show a decrease in fiber formation.

The plot of L/D as a function of the extrusion ratio is presented in figure 15. These results show that, as the extrusion ratio for zirconium oxide - columbium composites was increased from 16:1 to 24:1, the fiber L/D increased markedly. A further increase in the extrusion ratio to 32:1 resulted in only a slight increase in the L/D of the fiber.

The composites in which thorium oxide was fibered in columbium showed considerable change in L/D when the extrusion ratio was increased. Doubling the extrusion ratio from 16:1 to 32:1 resulted in a fivefold increase in the L/D of the fibers. Composites composed of magnesium oxide in tantalum show no increase in the fiber L/D with increase extrusion ratio.

Results of L/D determinations of the fibered oxides produced by hot rolling are given in table III and are shown in figure 16 as a function of the rolling temperature and the reduction in area. The change in L/D of the oxide fibers during hot rolling in a columbium or tantalum matrix was relatively small. Hot-rolled composites in which tungsten was the matrix exhibit a twofold increase in the fiber L/D when they are reduced from 50 to 75 percent at 3500°F ; and they show almost as great an increase

in fiber L/D when they are rolled at 3800° F.

Tensile Strength

The results of tensile tests conducted on the various oxide-metal composites are presented in table IV. The results of the room-temperature and elevated-temperature tensile tests conducted on zirconium oxide - columbium composites containing 17 and 20 volume percent oxide are presented in figure 17. These results show that at all test temperatures the oxide-metal composites exhibit tensile strengths considerably higher than the additive-free columbium, the greatest difference being observed at room temperature.

The results of tensile tests on thorium oxide - columbium composites are tabulated in table IV and are shown in figure 18. At room temperature, the composites exhibited a tensile strength of 106 000 pounds per square inch, whereas the additive-free columbium exhibited a tensile strength of 85 500 pounds per square inch. Comparison of the tensile strengths of the fibered composites reveals little difference between the properties of one composite and those of another composite of the same composition, even though the latter was processed under different extrusion conditions.

The results of tensile tests conducted on composites containing 20-volume-percent aluminum oxide in a matrix of columbium are presented in table IV and are plotted in figure 19. At all temperatures, the average ultimate tensile strengths of the composites containing unfibered oxides were almost the same as that of the additive-free columbium.

Stress-Rupture Results

The results of stress-rupture tests conducted on all oxide-metal composites are given in table V. In figure 20 are plotted the data for stress-rupture tests run at 2200° F on composites of zirconium oxide - columbium, and figure 21 shows the results of tests run at 2500° F. The composites tested at 2200° F exhibit a 1-hour life at an average stress of 20 200 pounds per square inch. For 10 hours of stress-rupture life, the composite average stress is 13 900 pounds per square inch; for 100 hours of life, the average stress is 7500 pounds per square inch. In general, the average stress necessary to cause failure of zirconium oxide - columbium composites at 2200° F was about three times that necessary to cause failure of the additive-free columbium. At

2500⁰ F, the stress required to cause rupture of the zirconium oxide - columbium composites in 1 hour averaged 7100 pounds per square inch; and the stresses required to cause rupture in a 10-hour and a 100-hour life were 5200 and 3500 pounds per square inch, respectively. At 2500⁰ F, the composites are approximately twice as strong as the additive-free metal.

Data for thorium oxide - columbium composites are given in table V and are plotted in figure 22 for tests run at 2200⁰ F and in figure 23 for tests run at 2500⁰ F. At 2200⁰ F the stress to cause rupture of the composites in 1 hour averaged 13 600 pounds per square inch, and the stress to cause rupture in 10 and 100 hours averaged 10 300 and 6900 pounds per square inch, respectively. Tests run at 2500⁰ F show that thorium oxide - columbium composites require an average stress of 7300 pounds per square inch to cause rupture in 1 hour while the required average stress to cause rupture in 10 and 100 hours was 5200 and 3100 pounds per square inch, respectively.

Microhardness

Listed in table VI are the results of microhardness tests conducted on the additive-free columbium, as well as on the columbium matrix and zirconium oxide fibers in composites, before and after heat treatment for 100 hours at 2200⁰ F in vacuum. A comparison of the rather limited data reveals that the hardness of the fibers in the as-extruded sample is considerably higher than that of the matrix. After heat treatment, the fibers are still harder than the matrix, but they appear to decrease in hardness more rapidly than does the matrix metal. The hardness of the additive-free columbium, both before and after heat treatment, was nearly the same as that of the columbium in the composites.

DISCUSSION

Fibering

Fibered oxide composites were produced by the in situ fibering of oxide particles in the ductile refractory metals columbium and tantalum. Zirconium oxide in columbium, thorium oxide in columbium, and magnesium oxide in tantalum fibered. Varying the extrusion temperature and the extrusion ratio influenced the degree of fibering. Thorium oxide fibering in columbium was observed at 0.57 and 0.63 of the oxide melting point, while the zirconium oxide in columbium was fibered at 0.65 to 0.78 of its melting point. Magnesium oxide in tantalum was fibered at 0.63 and 0.68 of the oxide melting point.

It was indicated previously in a compilation of hardness and modulus of elasticity data (refs. 8 and 15) that polycrystalline oxides soften at temperatures well below their melting point. Marked plastic deformation of oxides from equiaxed particles into fibers was obtained over a limited temperature range (ref. 6).

Although oxide fibering was achieved, the effect of temperature on the degree of fibering was not clearly established. Within the limited temperature range investigated, changing the extrusion temperature resulted in only small changes in the L/D of the fibers (fig. 14). The fact that the change in the L/D of the oxide with increased extrusion temperature was not consistent suggested that fibering may be related to the relative resistance of the materials to deformation at these extrusion temperatures. At low temperatures, the oxides would not be sufficiently ductile to be deformed, whereas at high temperatures, the matrix would become too soft to exert sufficient shear force on the oxide to cause deformation. Although the present investigation was not primarily concerned with establishing the limits of this temperature range, it is interesting that the extrusion temperatures utilized did result in oxide fibering.

A more pronounced effect on the L/D of the oxide fibers was obtained with changes in the extrusion ratio. Figure 15 shows that, in two out of three of the experiments run at a constant extrusion temperature, increasing the reduction ratio increased the L/D of the resulting fibers. This finding is similar to results observed for sodium chloride in copper (ref. 16). This increase in L/D appears to be related to the increase in hydrostatic and shear stresses to which the oxide is subjected during the higher reduction ratio extrusions.

A further indication of the importance of the relative resistance to deformation of matrix and oxide as related to oxide fibering, was obtained from the results of the hot-rolling experiments. As in the case of the extrusions, as the resistance to deformation of the matrix materials was changed, fibering of the ceramic was also changed. At 75 percent reduction, the L/D of zirconium oxide fibers in columbium was nearly the same whether they were rolled at 3500° or 3800° F. At the same reductions and temperatures, the zirconium oxide fibers in a tungsten matrix showed a marked increase in L/D (fig. 16). It would seem that the columbium is too soft at these temperatures to exert sufficient shear force to fiber the zirconium oxide particles. The tungsten resistance to deformation, however, is sufficiently greater than that of the oxide; therefore, the tungsten can exert shear force to deform the zirconium oxide particles.

Although the temperature and the amount of working (extrusion ratio or percent reduction) are important considerations in oxide fibering, many other variables may also have a bearing on the degree of oxide fibering. Typical variables are particle size, extrusion die angle, lubrication, can configuration, and ram speed. These variables, however, were not investigated in this study.

In addition to the aforementioned variables, the crystal structure of the oxide to be

fibered also seems to be important. In this investigation, the oxides that exhibited fibering were cubic at the extrusion temperature. The only oxide that did not fiber, even over a wide range of extrusion temperatures and extrusion ratios, was aluminum oxide, whose crystal structure is close packed hexagonal.

A similar tendency for cubic oxides to deform during the high-temperature working of a composite was reported in reference 17, where barium oxide, calcium oxide, cerium oxide, strontium oxide, and thorium oxide, all cubic, deformed when rolled in a molybdenum matrix. Reference 16 also reports the relative ease with which cubic ionic solids were deformed over a wide range of temperatures. Based on the results of the present study and on those of the other investigations, it is suggested that cubic oxides present the best possibility for fibering, probably because of the large number of possible slip systems that can operate during deformation. In hexagonal oxides, however, the possible number of operable slip systems is limited.

It might be argued that what appear to be fibers are nothing more than elongated clusters of unbonded oxide particles oriented in the direction of maximum working. Evidence to the contrary is presented in figure 24, which shows an electron photomicrograph of a zirconium oxide fiber in a columbium matrix. The ceramic particles used as the starting material were equiaxed. Examination of the microstructure of the fibers shows them to be composed of elongated grains whose major axes are parallel to the longitudinal axis of the fiber. This orientation would indicate that the oxide was plastically deformed during extrusion.

Evidence to indicate that the fibers are not clusters of disjointed particles is presented in figure 25. The specimen shown is one in which the columbium metal matrix was digested from around the oxide fibers to leave them exposed and unsupported. Minor deflections of the fiber were accomplished without causing them to fracture, indicating that the fibers possessed some degree of strength. Since fibers of sufficient length could not be recovered for mounting and testing in a whisker-tensile machine, no actual measure of the fiber strength was made.

Tensile Strength

Results obtained in this investigation revealed that incorporating fibers of a relatively inert, high-melting-point oxide in a ductile refractory-metal base can result in composites that exhibit tensile strengths considerably above those of the additive-free metal. Although the results show these improved tensile strengths, the mechanism by which the improvements are achieved can only be determined indirectly.

Investigators in the field of fiber metallurgy generally believe that several conditions must be met in order to attain desirable fiber composite properties. The modulus

of elasticity of the fiber should be equal to or greater than the modulus of the matrix for most tensile applications, and the creep rate of the fiber should be less than that of the matrix for creep-rupture applications. A good bond should exist between the matrix and the fiber, and the L/D of the fiber should be greater than a certain critical value. It is also necessary that the quantity of fibers in the composite be greater than a certain critical amount.

The aforementioned conditions may have been met in those oxide-fiber - metal composites that showed an improved tensile strength. The modulus of elasticity of the oxide was chosen to be greater than that of the matrix, as was pointed out in the section Materials Selection. Generally, the creep rate of oxides is much less than that of metals in the temperature range where the ceramic-metal composites were tested. The existence of what appeared to be a good bond between the fiber and the matrix is shown in the electron micrographs (fig. 24(a)). Although no estimate could be made of the L/D of the oxide fibers necessary for reinforcement, there are some indications that sufficient fibering may have been achieved. In those specimens exhibiting a large increase in tensile strength, fibering of the oxide had taken place (zirconium oxide and thorium oxide - columbium composites). In those specimens where no fibering of the oxides was observed (aluminum oxide - columbium composites), only a very small increase in tensile strength was obtained.

Work hardening, dispersion strengthening, and alloying could also account for some of the increase in strength of the fibered-oxide - metal composites, but it is felt that this was a secondary effect. The extrusion temperatures utilized were quite high, and whether significant amounts of strain energy would be retained in the metal after working at such high temperatures is doubtful. The particle size of the oxides was larger than is normally considered necessary for dispersion strengthening. Any alloying that may have taken place was probably due to oxygen contamination, a condition reflected in the high hardness of both the composite and the additive-free columbium (table VI). The oxygen content of the matrix was 3700 parts per million, which is quite high and would explain the high hardness. The hardness of the columbium in the composite indicates an oxygen level of about 6000 parts per million (ref. 18). The tensile strength of columbium at these levels (3700 compared with 6000 ppm) should not be appreciably different (ref. 18); however, the composite was still much stronger than the additive-free matrix.

A comparison of the tensile-strength - density ratio of the composites to that of several commercial columbium-based alloys is shown in figure 26. This plot shows that the composites are competitive with several commercial alloys (ref. 19), although their ratios were not as high as the Cb-20W-1Zr-0.1C alloy. In addition, the room-temperature ductility of the composites was low, although this may or may not have been due to the fibers since ductility of the additive-free columbium was also low. The

low ductility was probably due to the high oxygen level of both the composites and the additive-free matrix. The addition of an oxide to an alloy matrix was not attempted in this investigation but would be a logical extension in a future investigation.

Stress-Rupture

A comparison of the stress-rupture strength of additive-free columbium, zirconium oxide - columbium, and thorium oxide - columbium at 2200° and 2500° F is presented in figures 27 and 28. At both temperatures, the stress-rupture strength of the composites was better than that of the additive-free metal. These improvements were achieved with no increase in density and, in the case of the zirconium oxide - columbium composites, were achieved at a density less than that of the base material.

The relative stress-rupture strength of the composites and the columbium alloys is shown in figure 29, where the stress required to cause rupture in 10 hours at 2200° and 2500° F is compared. As was the case for tensile-strength - density ratio, the properties of the composites compared favorably with the commercial alloys but not with the Cb-20W-1Zr-0.1C alloy (ref. 19).

Some indication of a possible correlation between stress-rupture strength and the L/D of the oxide fibers in composites is seen in figure 30. The composites containing fibers having the higher L/D exhibit stress-rupture strengths superior to those composites in which the L/D of the fiber is smaller. Since other variables such as extrusion temperature were not held constant for the data shown, a quantitative correlation of rupture strength and L/D was unwarranted. It appears, however, that greater rupture strength was associated with a greater L/D.

CONCLUSIONS

Composites were produced that had a structure of elongated oxide fibers in refractory-metal matrices. From an investigation of the mechanical properties of these composites and from the techniques used to fabricate them, the following conclusions were drawn:

1. Oxides of magnesium, thorium, and zirconium were plastically deformed in refractory-metal matrices by mechanical working at temperatures from 0.57 to 0.78 of their respective melting points.
2. The fibering of the oxide by either hot rolling or extrusion was dependent upon the amount of deformation and the deformation temperature and was related to the crystal structure of the oxide.

3. The extent to which the oxides fibered was dependent upon the working temperature, the amount of deformation, and the relative resistance to deformation of the oxide and the surrounding matrix. For example, at a given reduction in area in rolling at 3800° F, there was greater deformation of zirconium oxide particles in a tungsten matrix than in a tantalum or columbium matrix.

4. The tensile strength, tensile-strength - density ratio, and stress-rupture strength of columbium containing fibered oxides were better than those of the additive-free columbium. These properties of the composites compared favorably with those of some commercial alloys.

Lewis Research Center,
National Aeronautics and Space Administration,
Cleveland, Ohio, November 28, 1966,
129-03-09-01-22.

REFERENCES

1. McDanel, David L.; Jech, Robert W.; and Weeton, John W.: Stress-Strain Behavior of Tungsten-Fiber-Reinforced Copper Composites. NASA TN D-1881, 1963.
2. Sutton, Willard H.; and Chorne, Juan: Development of High-Strength, Heat-Resistant Alloys by Whisker Reinforcement. ASM Metals Eng. Quart., vol. 3, no. 1, Feb. 1963, pp. 44-51.
3. Cratchley, D.; and Baker, A. A.: The Tensile Strength of Silica-Fibre-Reinforced Aluminum Alloy. Metallurgia, vol. 69, no. 414, Apr. 1964, pp. 153-159.
4. Otto, W. H.: Properties of Glass Fibers at Elevated Temperatures. Composite Materials and Composite Structures. Proceedings of the 6th Sagamore Ordnance Materials Research Conference, Racquette Lake, New York, Aug. 18-21, 1959. Rep. No. MET 661-601, Syracuse University Research Institute, 1959, pp. 277-303.
5. Arridge, R. G. C.; Baker, A. A.; and Cratchley, D.: Metal Coated Fibres and Fibre Reinforced Metals. J. Scientific Instr., vol. 41, May 1964, pp. 259-261.
6. Quantinetz, Max; Weeton, John W.; and Herbell, Thomas P.: Studies of Tungsten Composites Containing Fibered or Reacted Additives. NASA TN D-2757, 1965.
7. Shaffer, Peter T. B.: Handbook of High Temperature Materials - Materials Index. Plenum Press, 1964.

8. Hoffman, George A.; and Knapp, William J.: On the Linear Relation Between the Softening Temperature and the Melting Point of Ceramics. Rep. No. RM-2263, Rand Corp, Oct. 1, 1958. (Available from DDC as AD-206554.)
9. Coughlin, James P.: Contributions to the Data on Theoretical Metallurgy. XII - Heats and Free Energies of Formation of Inorganic Oxides. Bull. No. 542, U. S. Bureau of Mines, 1954.
10. Kingery, W. D.: Oxides for High-Temperature Applications. Proceedings of an International Symposium on High Temperature Technology, McGraw-Hill Book Co., Inc., 1960, pp. 76-89.
11. Samsonov, G. V.: Handbook of High Temperature Materials - Properties Index. Plenum Press, 1964.
12. Gyorgak, Charles W.: Extrusion at Temperatures Approaching 5000⁰ F. NASA TN D-3014, 1965.
13. Sikora, Paul F.; and Hall, Robert W.: High-Temperature Tensile Properties of Wrought Sintered Tungsten. NASA TN D-79, 1959.
14. Sikora, Paul F.: High-Temperature Tensile and Stress-Rupture Properties of Some Alloys in the Tungsten-Molybdenum System. NASA TN D-1087, 1962.
15. Wachtman, John B. Jr.; and Maxwell, Laurel H.: Factors Controlling Resistance to Deformation and Mechanical Failure in Polycrystalline (glass free) Ceramics. (WADC TR 57-526), National Bureau of Standards, Dec. 1957.
16. Warrick, R. J.; and Van Vlack, L. H.: Plastic Deformation of Non-Metallic Inclusions Within Ductile Metals. ASM Trans., vol. 57, 1964, pp. 672-689.
17. Bruckhart, W. L.; Craighead, C. M.; and Jaffee, R. I.: Investigation of Molybdenum and Molybdenum-Base Alloys Made by Powder-Metallurgy Techniques. (WADC TR 54-398), Battelle Memorial Inst., Jan. 1955.
18. Sisco, Frank T.; and Epremian, Edward, eds.: Columbium and Tantalum. John Wiley and Sons Inc., 1963.
19. Schmidt, F. F.; and Ogden, H. R.: The Engineering Properties of Columbium and Columbium Alloys. DMIC Rep. 188, Battelle Memorial Inst., Sept. 6, 1963.

TABLE I. - SUMMARY OF EXTRUSION BILLETS AND PROCESSING CONDITIONS

[Billets sintered in vacuum.]

Billet	Nominal composition				Sintering con- ditions		Density			Extrusion conditions				Density		
	Metal	Vol. % metal	Oxide	Vol. % oxide	Time, hr	Tempera- ture, °F	Sintered, g/cc	Calculated, g/cc	Percent of calculated	Billet diameter, in.	Tempera- ture, °F	Ratio		Extruded, g/cc	Percent of calculated	
												Nominal	Actual			
CZ-1 CZ-2 CZ-3 CZ-4 CZ-5 CZ-6 CBT-1	Columbium	80	Zirconium oxide	20	4	3700	7.33	7.93	92.4	3	3800	20	19.4	8.10	102	
		83	→	17	→	→	7.38	8.03	91.9	3	3500	24	24.1	8.10	101	
		83		17	→	→	7.35	8.03	91.5	3	3500	32	31.7	8.14	101	
		80		20	→	→	7.56	7.93	95.2	2	3500	20	17.9	8.31	103	
		80		20	→	→	7.53	7.93	94.9	2	3200	→	16.8	8.29	103	
		83		17	→	→	7.43	8.03	92.5	3	3500	19.4	8.04	100		
	100	-----	--	→	→	8.09	8.55	94.6	3	3500	→	19.1	8.57	100		
	CT-1 CT-2 CT-3 CT-4 CBT-1	Thorium oxide	80	20	→	4	3700	7.90	8.84	89.4	2	3500	16	16.7	8.83	99.6
			→	→	→	7.88	→	89.1	2	3200	16	16.9	8.79	99.4		
			→	→	→	7.46	→	85.0	3	→	32	30.5	8.82	99.8		
100			-----	--	→	→	7.42	→	84.5	3	→	32	33.2	8.78	99.3	
CA-3 CA-4 CA-5 CA-6 CA-7 CA-8 CA-9 CBA-1	Aluminum oxide	80	20	→	4	3300	6.94	7.58	91.6	2	→	--	→	→	→	
→		→	→	→	→	6.98	→	92.1	2	3000	8	8.6	→	→		
→		→	→	→	→	6.41	→	84.5	3	→	--	→	→			
→		→	→	→	→	6.67	→	87.9	3	→	--	→	→			
→		→	→	→	→	6.44	→	85.2	3	3200	20	19.9	→	→		
→		→	→	→	→	6.53	→	85.9	2	2500	16	17.0	→	→		
→		→	→	→	→	6.55	→	85.8	2	2800	16	17.3	→	→		
100		-----	--	→	→	7.61	8.55	89.0	3	3500	32	31.8	→	→		
TM-1 TM-2 TM-4 TM-5 TM-6 TM-7 TAM-1	Tantalum	80	Magnesium oxide	20	4	2900	10.1	14.0	72.3	2	3500	16	16.1	13.5	96.6	
		→	→	→	→	→	10.4	→	74.5	2	3200	16	19.1	14.9	107	
		→	→	→	→	→	11.0	→	78.7	2	3200	16	16.7	13.5	96.6	
		→	→	→	→	→	11.1	→	79.3	3	3500	24	23.8	13.3	95.2	
		→	→	→	→	→	11.3	→	80.6	→	→	--	→	→		
		→	→	→	→	→	11.2	→	80.2	→	→	--	→	→		
		100	-----	--	→	→	12.6	16.6	76.0	→	3500	24	24.0	16.4	98.7	
WR-2 WS-1 WS-2 WS-4 WS-5	Tungsten	80	Refrasil	20	4	2800	9.96	15.9	62.6	3	3000	8	8.7	→	→	
		→	Silicon dioxide	→	→	→	11.2	15.8	70.9	3	3000	8	8.0	→	→	
		→	→	→	→	→	10.8	→	68.3	3	3200	8	8.0	→	→	
		→	→	→	→	→	11.2	→	70.7	2	→	--	→	→		
		→	→	→	→	→	8.57	→	54.2	2	3200	8	8.5	→	→	
AG-1	Aluminum	80	Glass	20	4	1100	→	→	→	2	1100	16	15.8	→	→	

TABLE II. - MATERIALS ANALYSIS

Material	Particle size		Supplier's analysis		Final analysis, ppm
	Nominal	Measured, μm (a)	Material	Concentration	
Columbium	-325 Mesh	5	Carbon	500 ppm	430
			Nitrogen	500	390
			Oxygen	2000	3700
			Tantalum	1000 ↓	1500
Tantalum	-325 Mesh	15	Oxygen	450 ppm	600
			Carbon	30	80
			Nitrogen	180	390
			Iron	53	140
			Columbium	50 ↓	25
Aluminum oxide	-325 Mesh	11.3	Aluminum oxide	99.5 wt. %	----
Aluminum	-325 Mesh	-----	(b)	(b)	----
Thorium oxide	-325 Mesh	1.95	(b)	(b)	----
Silicon dioxide	10 μm	-----	Silicon dioxide	99.6 wt. %	----
Zirconium oxide	-325 Mesh	1.55	(b)	(b)	----
Alumina silicate	-----	10	Silicon dioxide	98.7 wt. %	----
			Aluminum oxide - ferrous oxide	1.0 wt. %	----
			Lime	.25 wt. %	----
Magnesium oxide	-----	0.4	Magnesium oxide	99.6 wt. %	----
Glass	-325 Mesh	37	(b)	(b)	----

^a Average particle size, Fisher subsieve size.

^b Analysis not available.

TABLE III. - LENGTH-DIAMETER RATIO OF FIBERED OXIDES

(a) Extruded composites

Billet	Composition				Extrusion conditions		Length-diameter ratio, L/D	
	Metal	Vol. % metal	Oxide	Vol. % oxide	Temperature, °F	Ratio		
CZ-1	Columbium ↓	80	Zirconium ↓	20	3800	19.4	11.1	
CZ-2		83		17	3500	24.1	8.4	
CZ-3		83		17	↓	31.7	9.0	
CZ-4		80		20		17.9	^a 4.5	
CZ-4		↓		↓		17.9	^b 6.5	
CZ-4		↓		↓		17.9	^c 4.1	
CZ-5		↓		↓	3200	16.8	5.9	
CZ-6		83		17	3500	19.4	4.6	
CT-1		80		20	3500	16.7	1.1	
CT-2		↓		↓	3200	16.9	1.6	
CT-3		↓		↓	↓	3200	30.5	9.0
CT-4						3200	33.2	19.3
TM-1	Tantalum	80	Magnesium	20	3500	16.1	10.4	
TM-2	Tantalum	80	Magnesium	20	3200	19.1	6.0	
TM-5	Tantalum	80	Magnesium	20	3500	23.8	5.7	

(b) Hot-rolled composites

Billet	Composition				Rolling conditions		Length-diameter ratio, L/D
	Metal	Vol. % metal	Oxide	Vol. % oxide	Temperature, °F	Reduction, percent	
CZR-1	Columbium	80	Zirconium	20	3500	25	-----
						50	-----
						75	2.2
						90	3.3
CZR-2	Columbium	80	Zirconium	20	3800	25	-----
						50	1.6
						75	2.7
TZR-1	Tantalum	80	Zirconium	20	3500	25	-----
TZR-2	Tantalum	80	Zirconium	20	3800	25	-----
						50	-----
						75	3.4
						90	2.9
WZR-1	Tungsten	80	Zirconium	20	3500	25	-----
						50	1.9
						75	5.1
						90	6.3
WZR-2	Tungsten	80	Zirconium	20	3800	25	-----
						50	2.4
						75	6.6

^aNose.^bMidsection.^cTail.

TABLE IV. - ROOM- AND ELEVATED-TEMPERATURE TENSILE PROPERTIES
OF COLUMBIUM COMPOSITES

Specimen	Composition			Test temperature, °F	Ultimate tensile strength, psi	Elongation, percent in 1" gage length	Reduction in area, percent
	Vol. % colum- bium	Oxide	Vol. % oxide				
CZ-1-18	80	Zirconium	20	Room temperature	136 800	11.0	1
CZ-1-12	↓	oxide	↓	1100	67 700	26.0	2
CZ-1-10	↓	↓	↓	2200	36 700	10.1	22
CZ-1-17	↓	↓	↓	2500	15 700	23.3	47
CZ-1-26	↓	↓	↓	2750	8 300	33.7	43
CZ-1-14	↓	↓	↓	3000	4 300	26.7	55
CZ-2-33	83	Zirconium	17	Room temperature	128 500	0.7	<1
CZ-2-27	↓	oxide	↓	1100	67 500	2.5	4
CZ-2-21	↓	↓	↓	2200	39 000	8.5	25
CZ-2-14	↓	↓	↓	2500	21 000	20.0	39
CZ-2-8	↓	↓	↓	2750	9 600	36.2	49
CZ-2-2	↓	↓	↓	3000	6 700	35.6	37
CZ-3-25	↓	↓	↓	Room temperature	140 700	1.2	1
CZ-3-31	↓	↓	↓	1100	67 700	2.9	3
CZ-3-7	↓	↓	↓	2200	38 300	10.8	22
CZ-3-4	↓	↓	↓	2500	14 500	30.8	57
CZ-3-10	↓	↓	↓	2750	8 400	51.7	53
CZ-3-3	↓	↓	↓	3000	4 100	21.7	56
CZ-4-12	80	Zirconium	20	Room temperature	110 000	----	<1
CZ-4-8	↓	oxide	↓	1100	67 800	1.5	1
CZ-4-14	↓	↓	↓	2200	35 500	6.3	15
CZ-4-13	↓	↓	↓	2500	17 700	17.5	33
CZ-4-7	↓	↓	↓	2750	7 300	43.8	54
CZ-4-2	↓	↓	↓	3000	5 300	40.5	47
CZ-5-2	↓	↓	↓	2500	10 150	40.9	45
CZ-5-8	↓	↓	↓	2500	10 370	35.6	48
CZ-5-12	↓	↓	↓	2500	10 900	41.7	53
CZ-6-12	83	Zirconium	17	Room temperature	99 500	2.0	<1
CZ-6-18	↓	oxide	↓	Room temperature	62 800	1.0	1
CZ-6-14	↓	↓	↓	1100	66 100	1.9	4
CZ-6-11	↓	↓	↓	2200	37 600	6.9	14
CZ-6-8	↓	↓	↓	2500	14 800	23.2	45
CZ-6-13	↓	↓	↓	2750	5 400	33.0	47
CZ-6-2	↓	↓	↓	3000	4 900	58.1	47

TABLE IV. - Concluded. ROOM- AND ELEVATED-TEMPERATURE TENSILE PROPERTIES
OF COLUMBIUM COMPOSITES

Specimen	Composition			Test temperature, °F	Ultimate tensile strength, psi	Elongation, percent in 1" gage length	Reduction in area, percent
	Vol. % colum- bium	Oxide	Vol. % oxide				
CBZ-1-23	100	None	0	Room temperature	64 100	0.4	<1
CBZ-1-13	↓	↓	↓	1100	57 400	5.6	4
CBZ-1-7	↓	↓	↓	2200	13 300	43.1	67
CBZ-1-4	↓	↓	↓	2500	5 400	81.6	92
CBZ-1-19	↓	↓	↓	2750	3 200	151.5	91
CBZ-1-6	↓	↓	↓	3000	2 100	94.1	100
CT-1-14	80	Thorium oxide	20	2200	27 400	19.0	37
CT-1-15	↓	↓	↓	2500	12 400	45.7	42
CT-2-16	↓	↓	↓	2200	25 900	22.7	50
CT-2-13	↓	↓	↓	2500	12 600	36.0	49
CT-3-8	↓	↓	↓	Room temperature	106 000	.4	<1
CT-3-11	↓	↓	↓	1100	63 900	.8	1
CT-3-14	↓	↓	↓	2200	22 200	14.1	35
CT-3-16	↓	↓	↓	2500	15 700	27.1	42
CT-3-18	↓	↓	↓	2750	11 100	24.0	40
CT-3-21	↓	↓	↓	3000	8 000	32.4	36
CBT-1-4	100	None	0	Room temperature	85 500	-----	---
CBT-1-10	↓	↓	↓	1100	65 600	6.4	6
CBT-1-17	↓	↓	↓	2200	12 500	50.5	76
CBT-1-26	↓	↓	↓	2500	5 100	108.7	100
CBT-1-32	↓	↓	↓	2750	3 200	146.3	100
CBT-1-33	↓	↓	↓	3000	2 000	104.5	100
CA-7-7	80	Aluminum oxide	20	2200	14 500	13.0	22
CA-7-18	↓	↓	↓	2500	10 700	17.1	18
CA-8-2	↓	↓	↓	2500	5 900	25.4	23
CA-8-8	↓	↓	↓	2500	6 900	27.0	21
CA-8-12	↓	↓	↓	2750	5 300	30.3	29
CA-9-10	↓	↓	↓	2200	12 475	21.6	23
CA-9-15	↓	↓	↓	3000	3 100	45.5	42
CBA-1-4	100	None	0	2200	15 500	45.8	98
CBA-1-6	↓	↓	↓	2500	5 200	91.1	100
CBA-1-3	↓	↓	↓	2750	3 200	117.4	100
CBA-1-7	↓	↓	↓	3000	600	-----	---

TABLE V. - STRESS-RUPTURE PROPERTIES OF COLUMBIUM COMPOSITES

AT 2200° AND 2500° F

Specimen	Composition			Test temperature, °F	Stress, psi	Life, hr	Elongation, percent in 1" gage length	Reduction in area, percent
	Vol. % colum- bium	Oxide	Vol. % oxide					
CZ-1-23	80	Zirconium	20	2200	8 000	119.0	28.4	33.2
CZ-1-13	↓	oxide	↓	2200	12 000	17.4	31.5	44.9
CZ-1-7	↓	↓	↓	2200	16 000	3.2	13.8	39.3
CZ-1-4	↓	↓	↓	2500	2 500	373.2	38.9	26.1
CZ-1-20	↓	↓	↓	↓	3 750	81.0	35.7	23.7
CZ-1-9	↓	↓	↓	↓	5 000	24.6	36.2	34.6
CZ-1-11	↓	↓	↓	↓	6 000	7.3	38.2	41.1
CZ-2-17	83	Zirconium	17	2200	8 000	59.5	40.3	52.4
CZ-2-11	↓	oxide	↓	↓	12 000	14.1	28.0	45.2
CZ-2-13	↓	↓	↓	↓	13 600	7.9	16.1	47.5
CZ-2-5	↓	↓	↓	↓	16 000	6.9	27.2	44.5
CZ-2-24	↓	↓	↓	2500	2 500	396.4	40.0	31.9
CZ-2-9	↓	↓	↓	↓	3 500	64.8	28.4	41.7
CZ-2-30	↓	↓	↓	↓	4 500	39.2	42.4	35.6
CZ-2-12	↓	↓	↓	↓	5 500	8.1	38.1	46.0
CZ-3-28	↓	↓	↓	2200	6 000	432.1	38.0	39.2
CZ-3-34	↓	↓	↓	↓	9 000	47.3	28.1	51.0
CZ-3-9	↓	↓	↓	↓	12 000	14.1	32.0	50.7
CZ-3-11	↓	↓	↓	↓	16 000	4.9	23.8	44.2
CZ-3-13	↓	↓	↓	2500	2 500	216.2	37.8	36.0
CZ-3-16	↓	↓	↓	↓	3 500	160.0	74.5	72.7
CZ-3-19	↓	↓	↓	↓	4 500	23.9	28.7	50.7
CZ-3-22	↓	↓	↓	↓	5 500	8.2	37.0	44.8
CZ-4-10	80	Zirconium	20	2200	8 000	117.7	38.9	49.8
CZ-4-9	↓	oxide	↓	↓	8 750	97.4	30.2	43.1
CZ-4-5	↓	↓	↓	↓	12 250	30.4	23.4	53.1
CZ-4-3	↓	↓	↓	↓	17 500	6.4	27.8	34.7
CZ-5-3	↓	↓	↓	2500	2 500	143.3	48.3	47.1
CZ-5-11	↓	↓	↓	↓	2 500	197.3	65.5	55.7
CZ-5-6	↓	↓	↓	↓	3 500	36.1	59.7	48.2
CZ-5-9	↓	↓	↓	↓	4 500	6.1	50.4	54.9
CZ-5-5	↓	↓	↓	↓	5 000	3.9	50.0	46.4
CZ-5-10	↓	↓	↓	↓	5 500	2.9	48.1	58.7
CZ-6-4	83	Zirconium	17	2200	5 900	191.7	23.5	51.2
CZ-6-22	↓	oxide	↓	↓	9 100	26.9	23.0	50.3
CZ-6-17	↓	↓	↓	↓	12 300	10.7	17.2	43.0
CZ-6-9	↓	↓	↓	↓	16 000	4.2	21.1	37.4
CZ-6-15	↓	↓	↓	2500	2 500	192.8	43.6	33.5
CZ-6-7	↓	↓	↓	↓	3 500	57.6	46.9	38.3
CZ-6-10	↓	↓	↓	↓	4 500	15.4	41.7	42.5
CZ-6-3	↓	↓	↓	↓	5 500	5.1	36.9	47.8

TABLE V. - Concluded. STRESS-RUPTURE PROPERTIES OF COLUMBIUM

COMPOSITES AT 2200° AND 2500° F

Specimen	Composition			Test temperature, °F	Stress, psi	Life, hr	Elongation, percent in 1" gage length	Reduction in area, percent
	Vol. % colum- bium	Oxide	Vol. % oxide					
CBZ-1-18	100	None	0	2200	2 500	169.9	87.5	97.5
CBZ-1-8	↓	↓	↓	↓	4 000	19.6	76.7	94.3
CBZ-1-3	↓	↓	↓	↓	5 000	6.8	82.1	94.5
CBZ-1-14	↓	↓	↓	↓	7 500	.8	32.5	90.5
CBZ-1-9	↓	↓	↓	2500	1 000	359.9	70.0	65.7
CBZ-1-15	↓	↓	↓	↓	2 000	20.0	105.5	93.8
CBZ-1-17	↓	↓	↓	↓	2 500	5.3	94.0	98.4
CBZ-1-29	↓	↓	↓	↓	3 000	1.1	57.9	72.1
CT-1-10	80	Thorium oxide	20	2500	2 500	125.4	23.6	-----
CT-1-6	↓	↓	↓	2500	6 000	1.8	21.3	-----
CT-1-11	↓	↓	↓	2200	6 000	96.4	34.2	52.4
CT-1-13	↓	↓	↓	↓	8 000	23.0	33.8	52.4
CT-1-8	↓	↓	↓	↓	10 000	9.4	33.3	45.8
CT-2-12	↓	↓	↓	↓	6 000	70.3	30.7	39.9
CT-2-14	↓	↓	↓	↓	8 000	19.8	38.8	48.7
CT-2-3	↓	↓	↓	↓	10 000	5.2	24.3	38.4
CT-2-10	↓	↓	↓	2500	4 000	8.0	23.9	-----
CT-2-6	↓	↓	↓	2500	4 900	3.3	19.6	-----
CT-2-9	↓	↓	↓	2500	6 500	.8	40.7	47.7
CT-3-4	↓	↓	↓	2200	6 000	715.2	25.0	36.8
CT-3-6	↓	↓	↓	↓	8 000	97.5	14.0	33.5
CT-3-13	↓	↓	↓	↓	9 000	33.6	13.4	36.8
CT-3-5	↓	↓	↓	↓	11 000	21.8	12.5	31.8
CT-3-3	↓	↓	↓	↓	13 000	4.1	9.7	27.6
CT-3-20	↓	↓	↓	2500	2 000	^a >1000	(a)	(a)
CT-3-7	↓	↓	↓	↓	5 000	74.2	20.0	23.6
CT-3-10	↓	↓	↓	↓	7 500	6.7	25.4	32.2
CT-3-2	↓	↓	↓	↓	9 000	1.4	17.3	31.8
CBT-1-34	100	None	0	2200	2 500	105.5	80.5	95.1
CBT-1-28	↓	↓	↓	↓	4 000	9.8	44.6	94.6
CBT-1-31	↓	↓	↓	↓	5 000	4.1	43.0	54.4
CBT-1-27	↓	↓	↓	↓	7 400	.5	31.2	88.2
CBT-1-14	↓	↓	↓	2500	1 000	107.3	89.4	98.5
CBT-1-25	↓	↓	↓	↓	1 500	24.5	66.3	92.5
CBT-1-20	↓	↓	↓	↓	2 000	8.5	105.6	100.0
CBT-1-29	↓	↓	↓	↓	3 000	1.5	151.3	100.0

^aTest stopped before failure.

TABLE VI. - ROOM-TEMPERATURE

MICROHARDNESS

[Load, 25 g.]

Hardness in composite specimen CZ-2, KHN		Hardness in additive- free columbium specimen CBZ-1, KHN
Metal	Oxide	
As extruded		
454	985	316
488	985	318
347	732	368
395	807	409
<u>423</u>	<u>814</u>	<u>343</u>
Average 421	865	351
Heat treated 100 hours at 2200 ⁰ F in vacuum		
327	807	316
395	807	303
370	672	298
327	889	316
347	672	305
—	—	<u>302</u>
Average 353	769	307

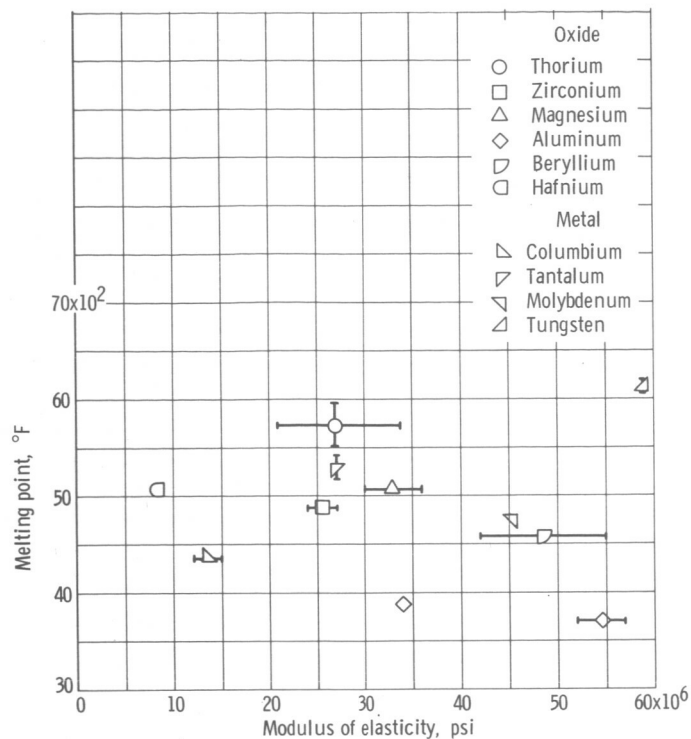
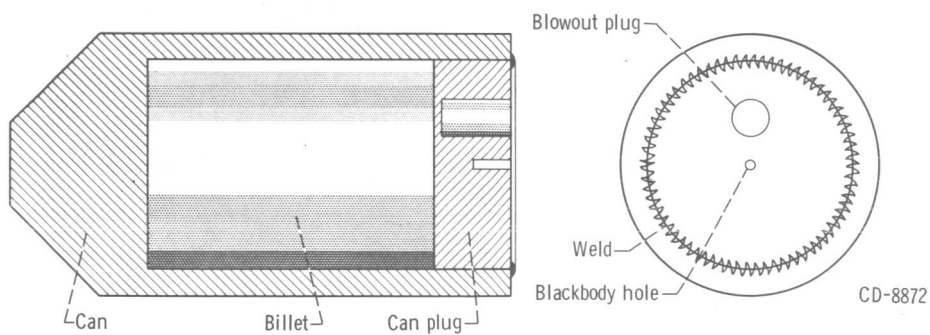
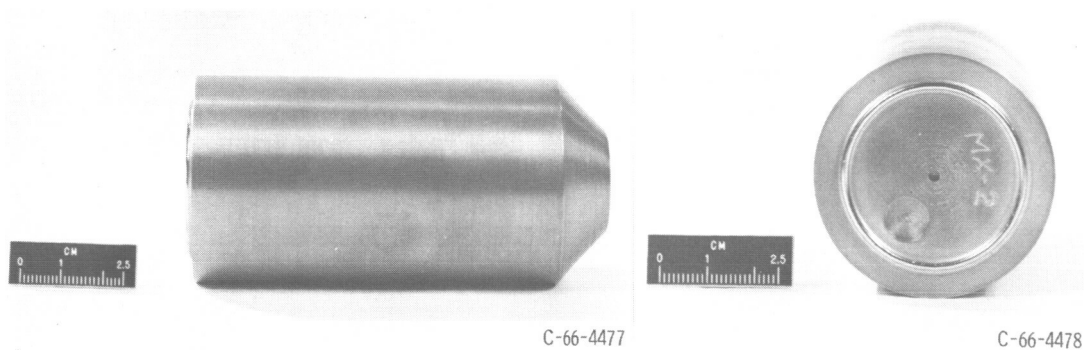


Figure 1. - Room-temperature modulus of elasticity and melting point of various metals and oxides (data from ref. 7).



(a) Diagram showing extrusion can and billet.



(b) Canned billet.

Figure 2. - Extrusion billet and can.

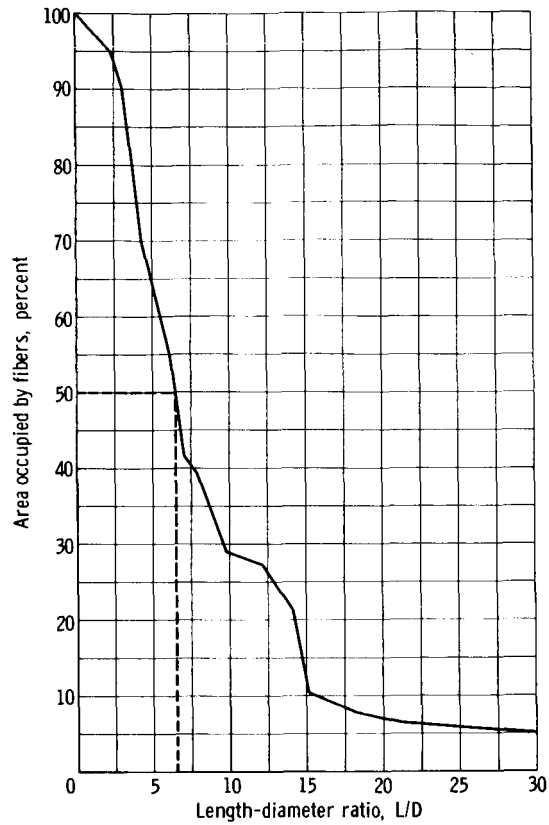


Figure 3. - Plot used to determine length-diameter ratio of oxide fibers in composites.

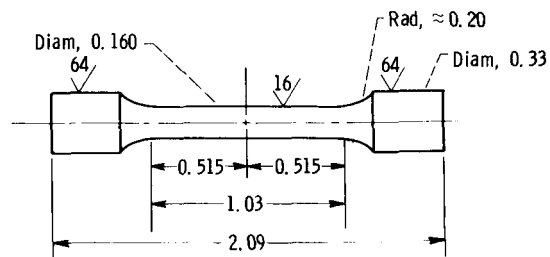
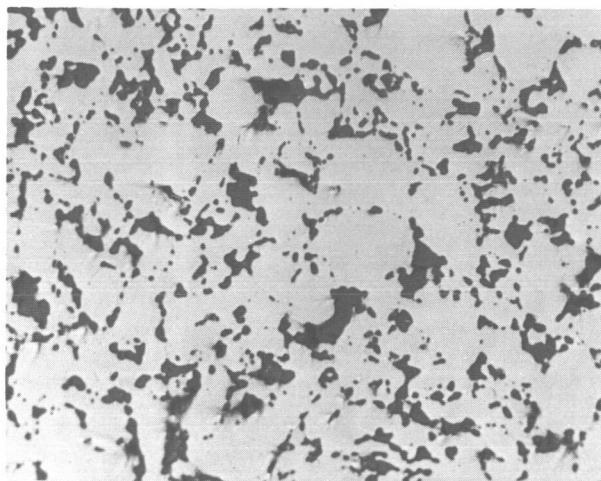
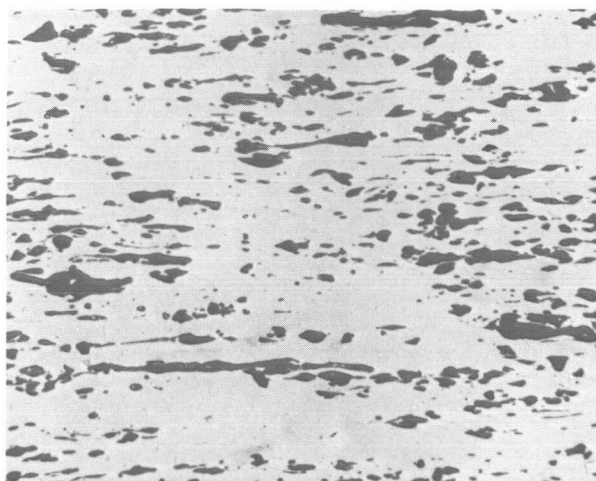


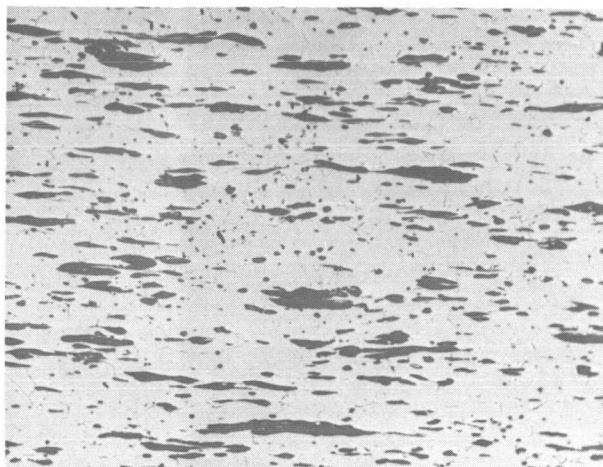
Figure 4. - Tensile and stress-rupture specimen (all dimensions in inches).



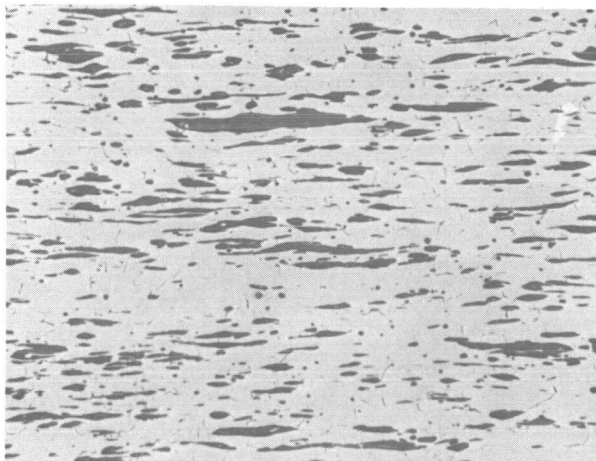
(a) Sintered; 20 volume percent zirconium oxide; longitudinal section.



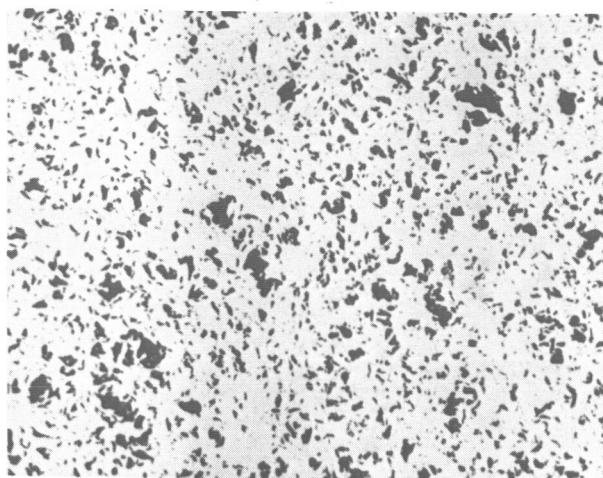
(b) Extruded; 20 volume percent zirconium oxide; extrusion ratio, 20; extrusion temperature, 3500° F; longitudinal section.



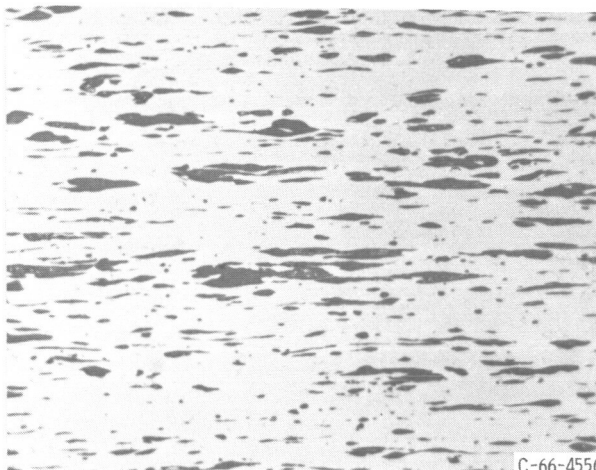
(c) Extruded; 20 volume percent zirconium oxide; extrusion ratio, 20; extrusion temperature, 3800° F; longitudinal section.



(d) Extruded; 17 volume percent zirconium oxide; extrusion ratio, 24; extrusion temperature, 3500° F; longitudinal section.



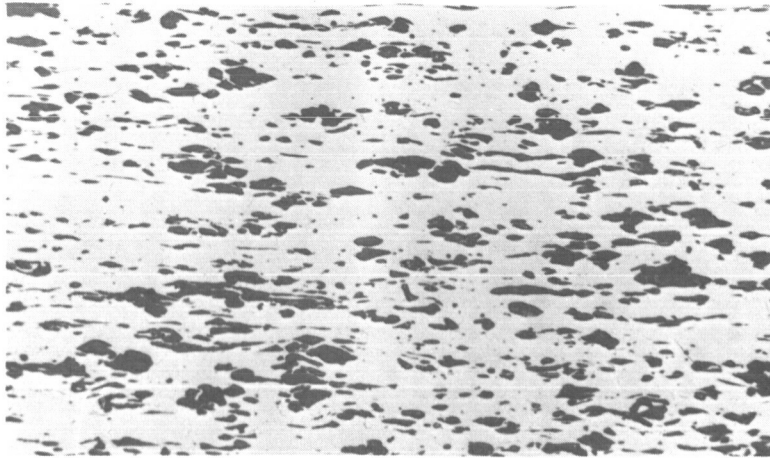
(e) Extruded; 20 volume percent zirconium oxide; extrusion ratio, 20; extrusion temperature, 3500° F; transverse section.



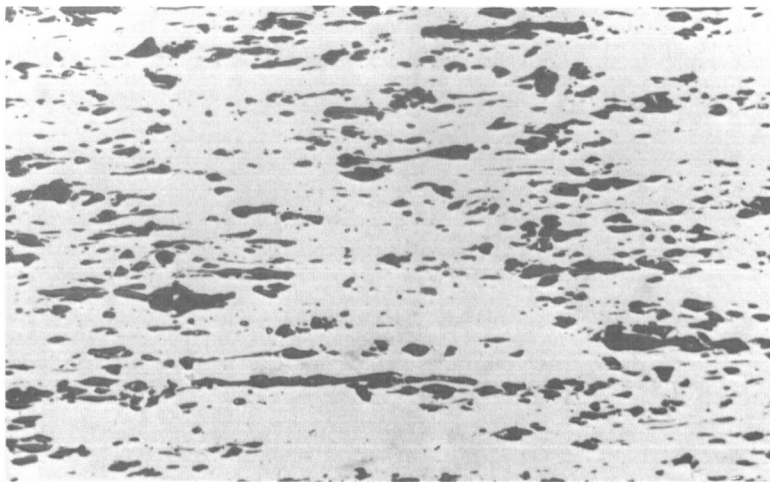
(f) Extruded; 17 volume percent zirconium oxide; extrusion ratio, 32; extrusion temperature, 3500° F; longitudinal section.

Figure 5. - Microstructure of as-sintered, sintered and extruded zirconium oxide - columbium composites; unetched. X250.

C-66-4556



(a) Nose section.



(b) Midsection.

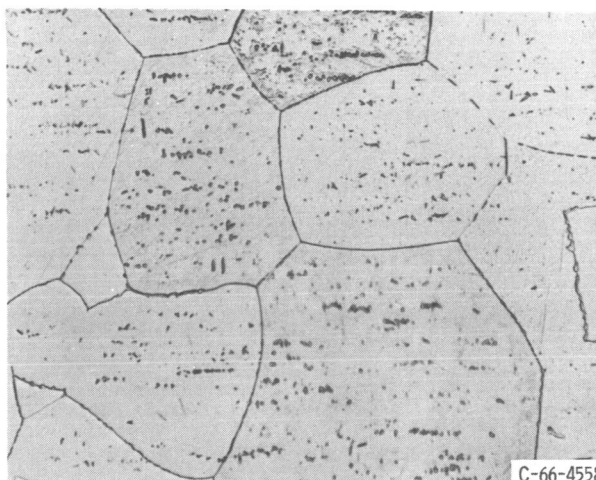


(c) Tail section.

Figure 6. - Microstructure of extruded zirconium oxide - columbium composites at various sections along extruded length; 20 volume percent zirconium oxide; extrusion ratio, 20; extrusion temperature, 3500° F; unetched; longitudinal sections. X250.



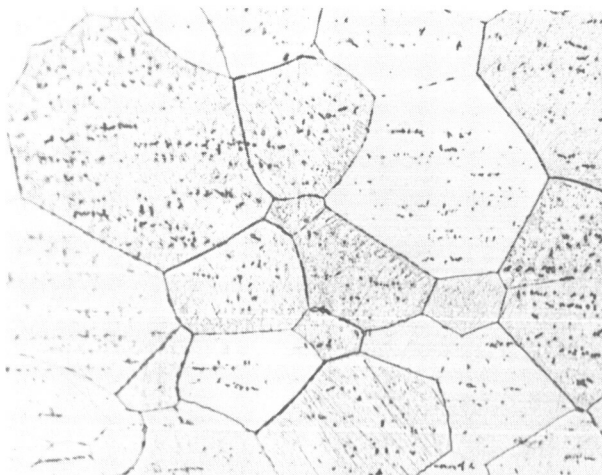
(a) Zirconium oxide-columbium composite; 17 volume percent zirconium oxide.



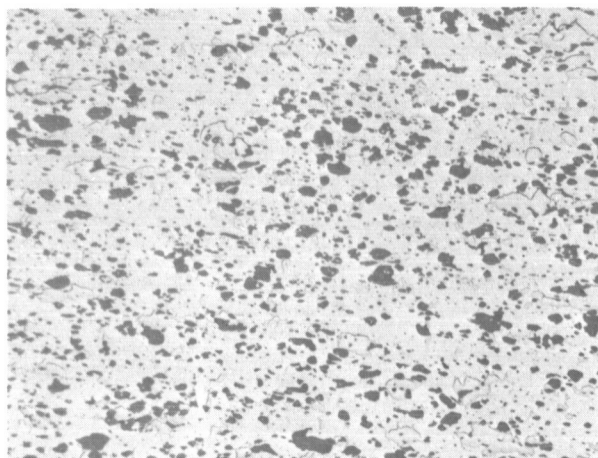
(b) Columbium.

C-66-4558

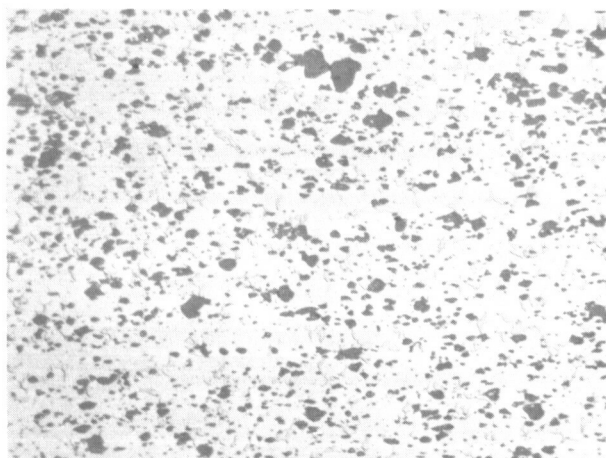
Figure 7. - Microstructures of extruded columbium and zirconium oxide - columbium composite; extrusion ratio, 20; extrusion temperature, 3500° F; etchant, 1 part hydrofluoric acid, 2 parts nitric acid, 3 parts water; longitudinal section. X250.



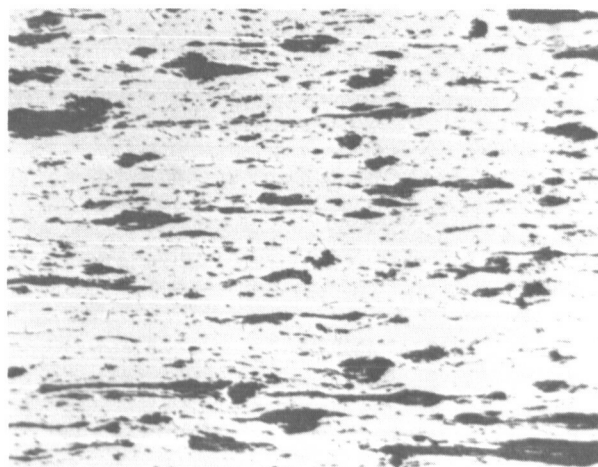
(a) Columbium; extrusion ratio 32; extrusion temperature, 3200° F; etchant, 1 part hydrofluoric acid, 2 parts nitric acid, 1 part water; longitudinal section.



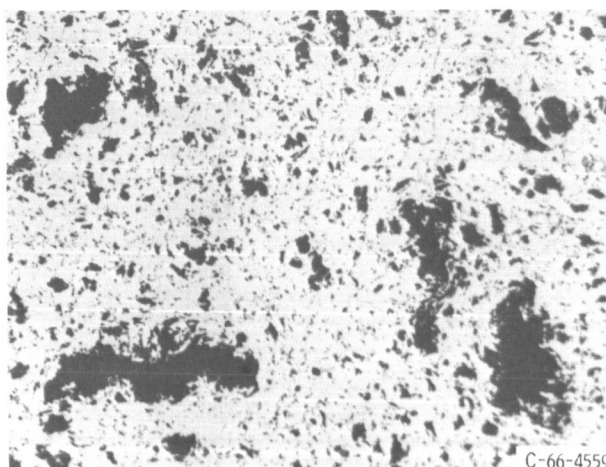
(b) Columbium - 20 volume percent thorium oxide; extrusion ratio, 16; extrusion temperature, 3200° F; unetched; longitudinal section.



(c) Columbium - 20 volume percent thorium oxide; extrusion ratio, 16; extrusion temperature, 3500° F; unetched; longitudinal section.

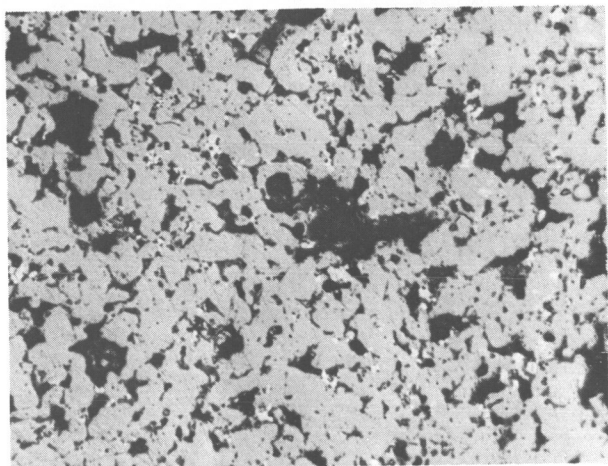


(d) Columbium - 20 volume percent thorium oxide; extrusion ratio, 32; extrusion temperature, 3200° F; unetched; longitudinal section.

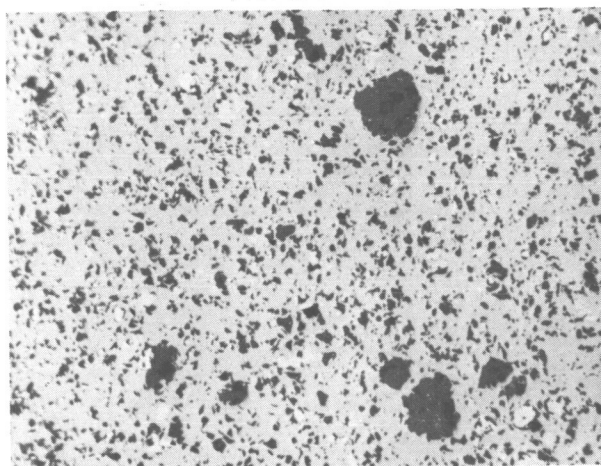


(e) Columbium - 20 volume percent thorium oxide; extrusion ratio, 32; extrusion temperature, 3200° F; unetched; transverse section.

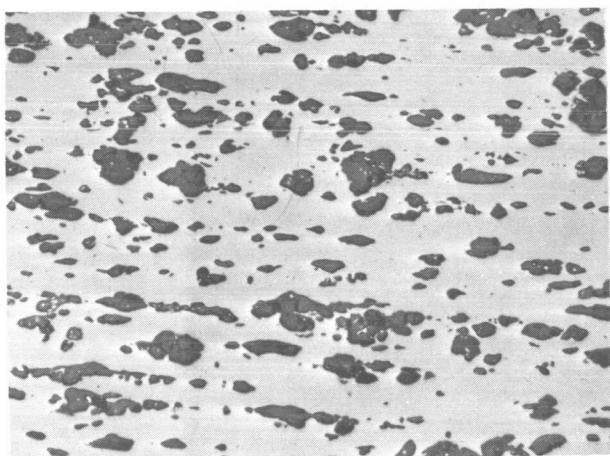
Figure 8. - Microstructures of extruded columbium and thorium oxide - columbium composites. X250.



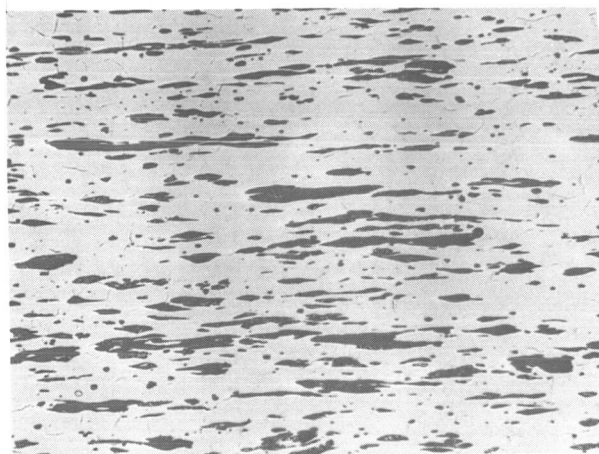
(a) As-sintered; sintering time 4 hours; sintering temperature, 2900° F; longitudinal section.



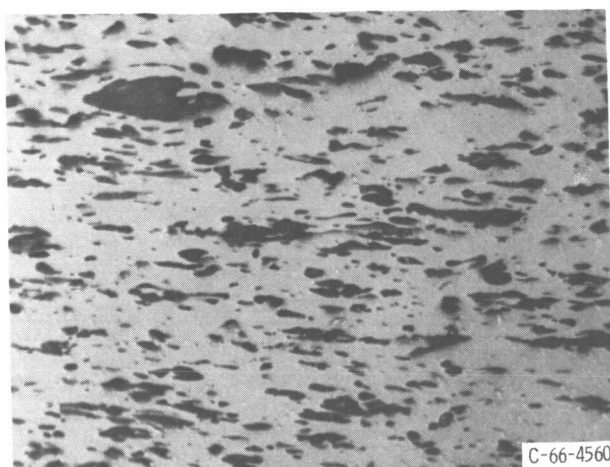
(b) Extruded; extrusion ratio, 24; extrusion temperature, 3500° F; transverse section.



(c) Extruded; extrusion ratio, 16; extrusion temperature, 3200° F; longitudinal section.

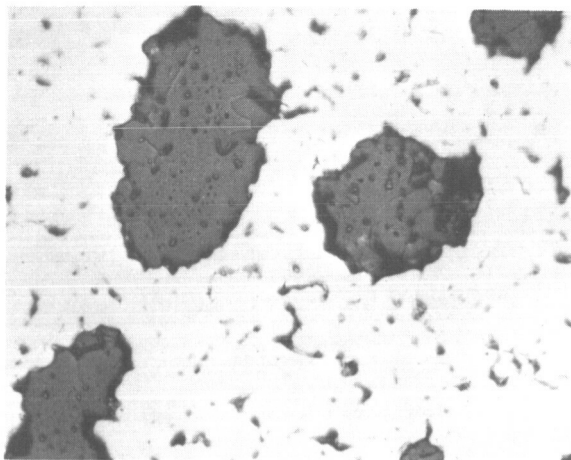


(d) Extruded; extrusion ratio, 16; extrusion temperature, 3500° F; longitudinal section.

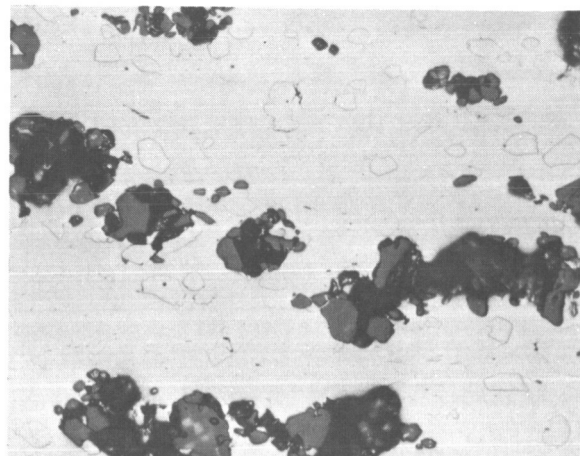


(e) Extruded; extrusion ratio, 24; extrusion temperature, 3500° F; longitudinal section.

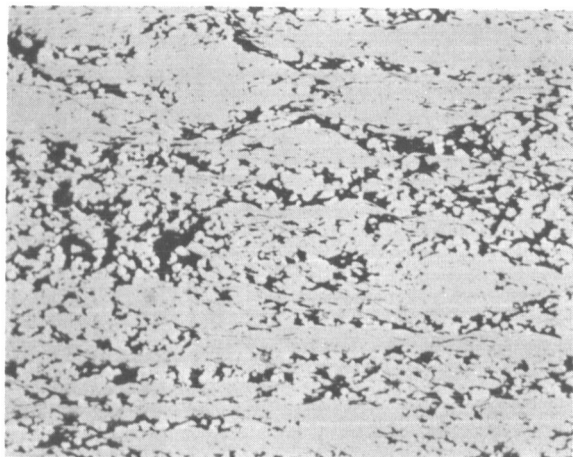
Figure 9. - Microstructures of as-sintered and extruded magnesium oxide - tantalum composites; unetched. X250.



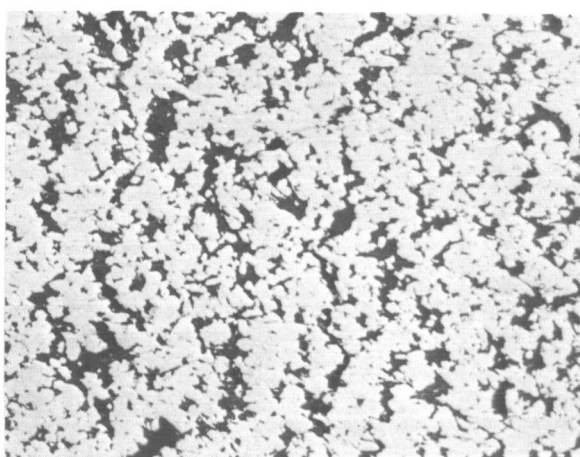
(a) As-sintered columbium - 20 volume percent aluminum oxide composite; sintering time, 4 hours; sintering temperature, 3300° F; longitudinal section.



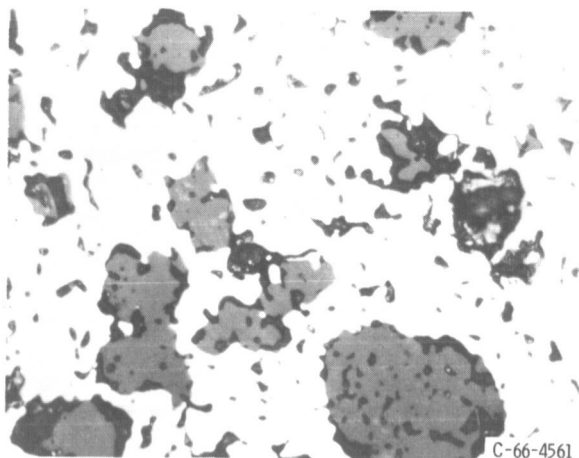
(b) Extruded columbium - 20 volume percent aluminum oxide composite; extrusion ratio, 8; extrusion temperature, 3000° F; longitudinal section.



(c) Extruded tungsten - 20 volume percent silicon dioxide; extrusion ratio, 8; extrusion temperature, 3000° F; longitudinal section.

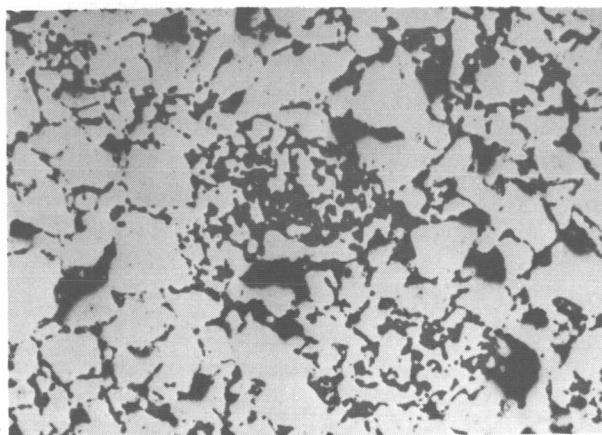


(d) Extruded tungsten - 20 volume percent silicon dioxide composite; extrusion ratio, 8; extrusion temperature, 3200° F; longitudinal section.

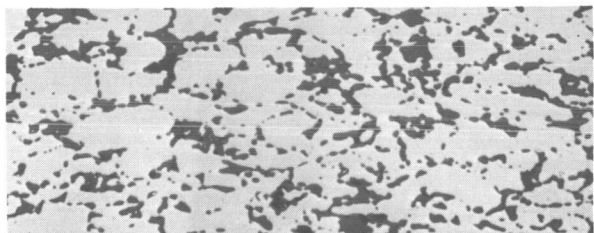


(e) Extruded aluminum - 20 volume percent glass composite; extrusion ratio, 16, extrusion temperature, 1100° F; longitudinal section.

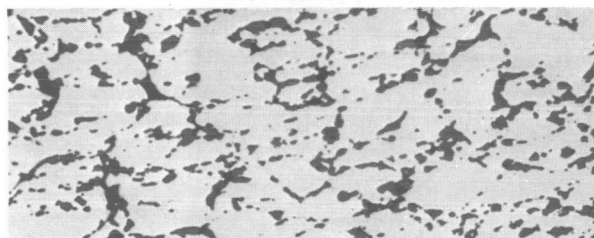
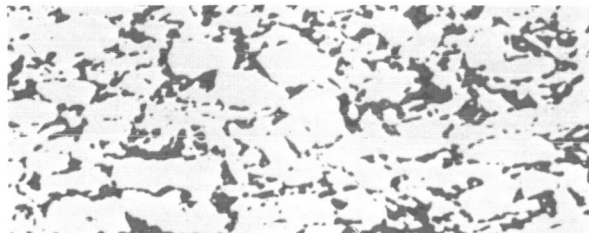
Figure 10. - Microstructures of as-sintered and extruded aluminum oxide - columbium, silicon dioxide - tungsten, and glass-aluminum composites; unetched. X250.



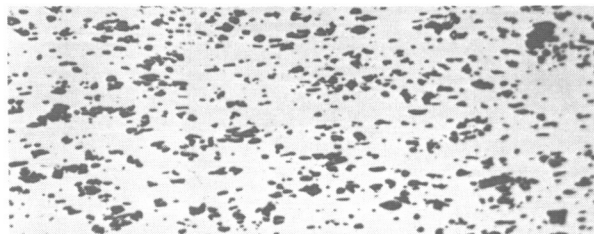
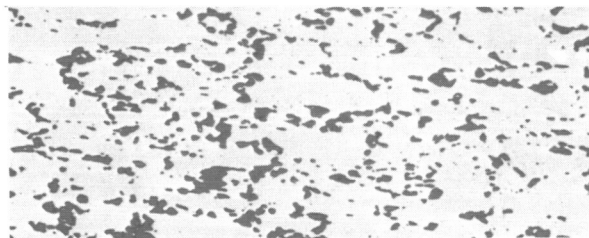
(a) As-sintered; sintering time, 4 hours; sintering temperature, 3700° F.
Reduction
ratio



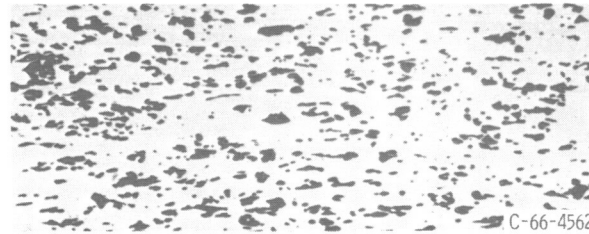
25%



50%

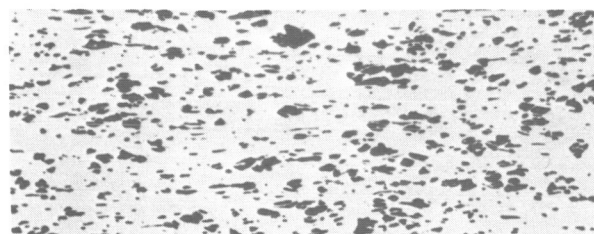


75%



C-66-4562

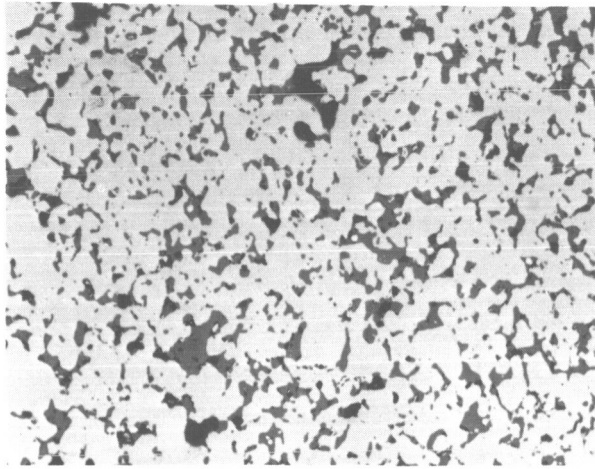
(c) Hot-rolled at 3800° F.



90%

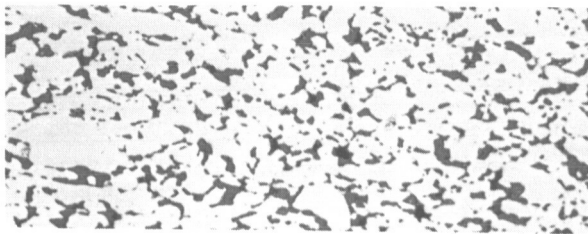
(b) Hot-rolled at 3500° F.

Figure 11. - Microstructures of as-sintered and hot-rolled zirconium oxide - columbium composites; 20 volume percent zirconium oxide; unetched; longitudinal sections. X250.



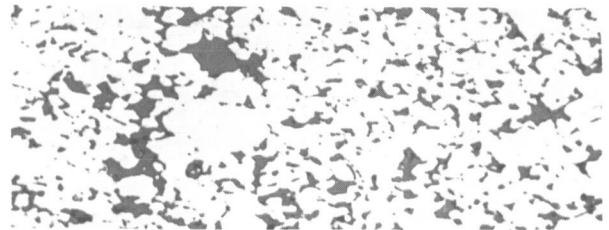
(a) As-sintered; sintering time, 4 hours; sintering temperature, 3700° F.

Reduction
ratio

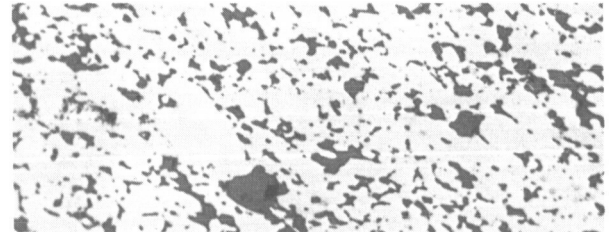


(b) Hot-rolled at 3500° F.

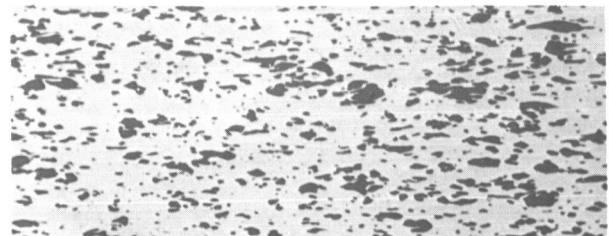
25%



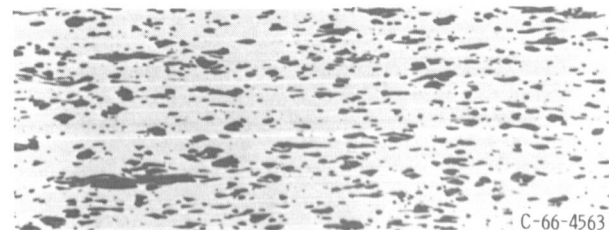
50%



75%



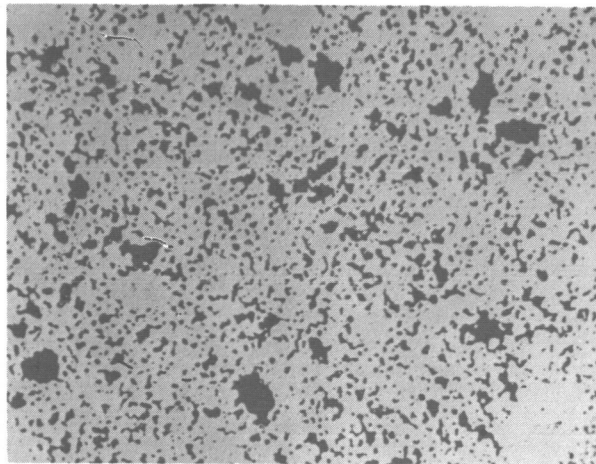
90%



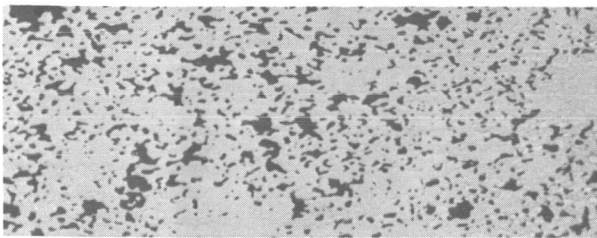
C-66-4563

(c) Hot-rolled at 3800° F.

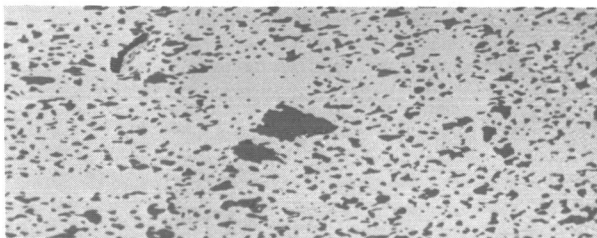
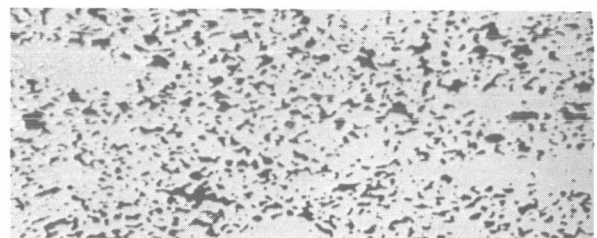
Figure 12. - Microstructure of as-sintered hot-rolled zirconium oxide - tantalum composites; 20 volume percent zirconium oxide; unetched; longitudinal sections. X250.



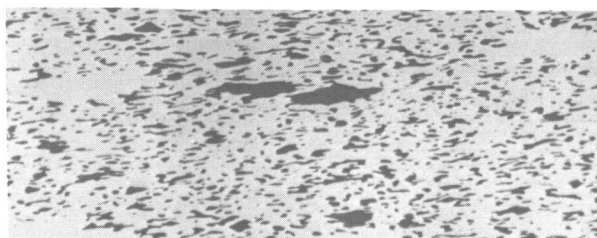
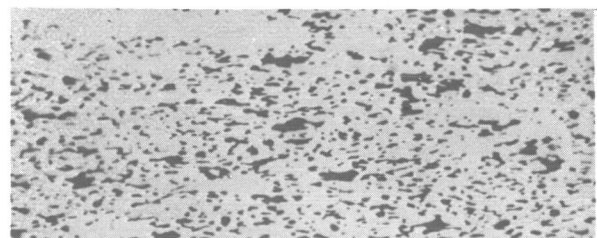
(a) As-sintered; sintering time 4 hours; sintering temperature, 4000° F.
Reduction
ratio



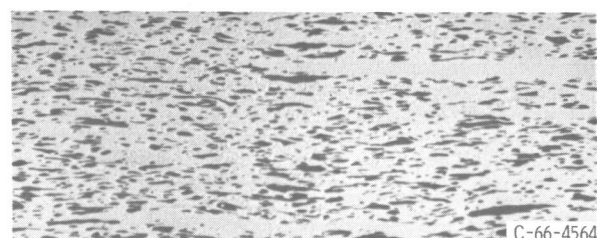
25%



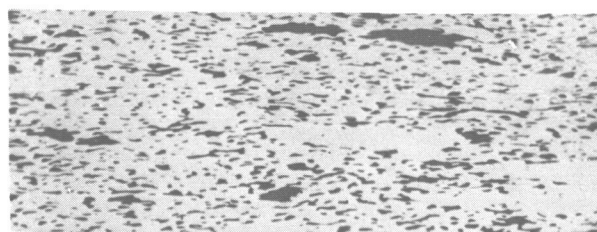
50%



75%



C-66-4564



90%

(c) Hot-rolled at 3800° F.

(b) Hot-rolled at 3500° F.

Figure 13. - Microstructure of as-sintered and hot-rolled zirconium oxide - tungsten composites; 20 volume percent zirconium oxide; unetched; longitudinal sections. X250.

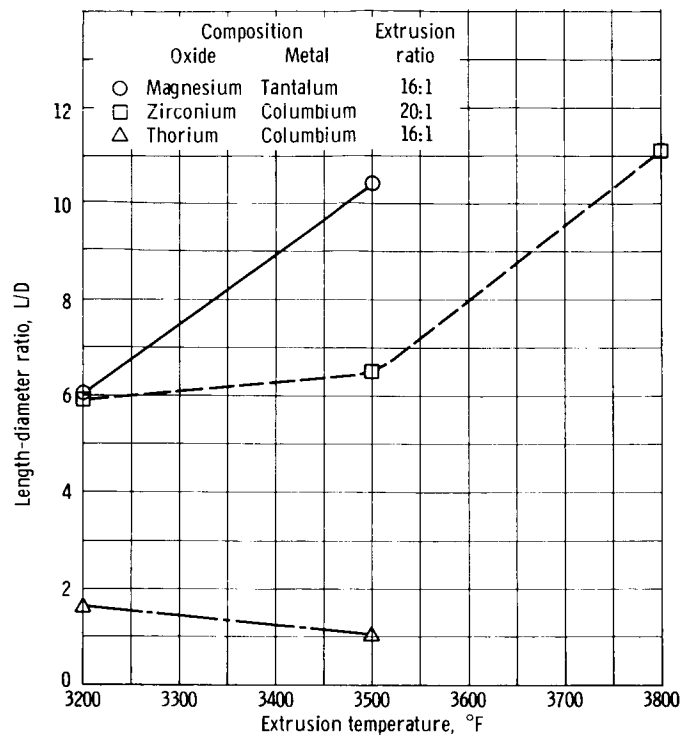


Figure 14. - Effect of extrusion temperature on length-diameter ratio of 20-volume-percent fibered oxides.

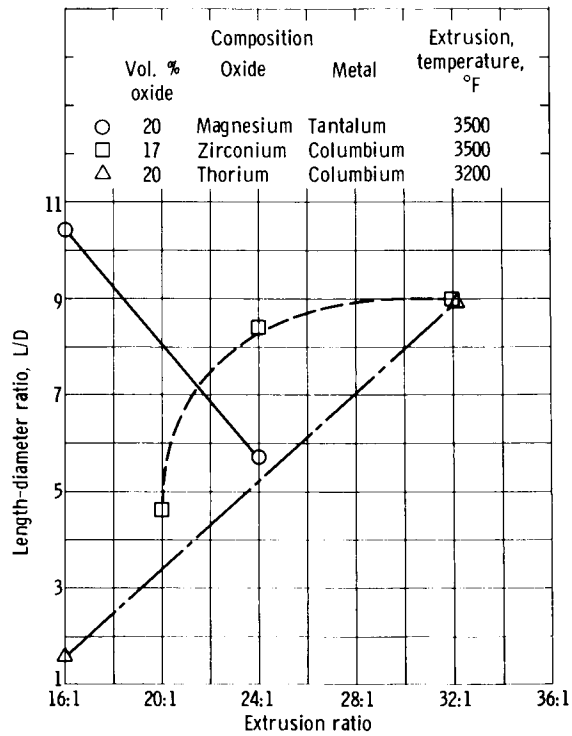


Figure 15. - Effect of extrusion ratio on length-diameter ratio of fibered oxides.

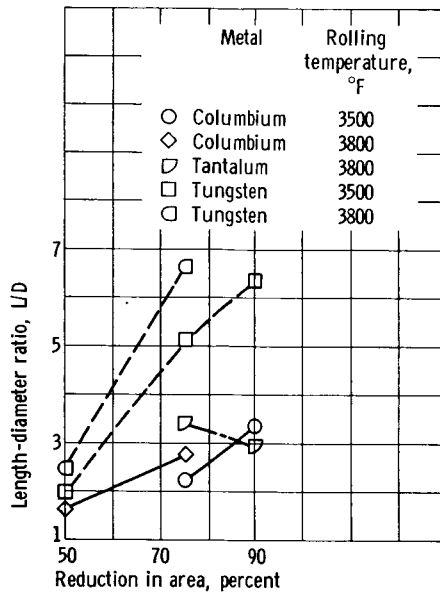


Figure 16. - Effect of rolling temperature and reduction on length-diameter ratio of fibered 20-volume-percent zirconium oxide in columbium, tantalum, and tungsten.

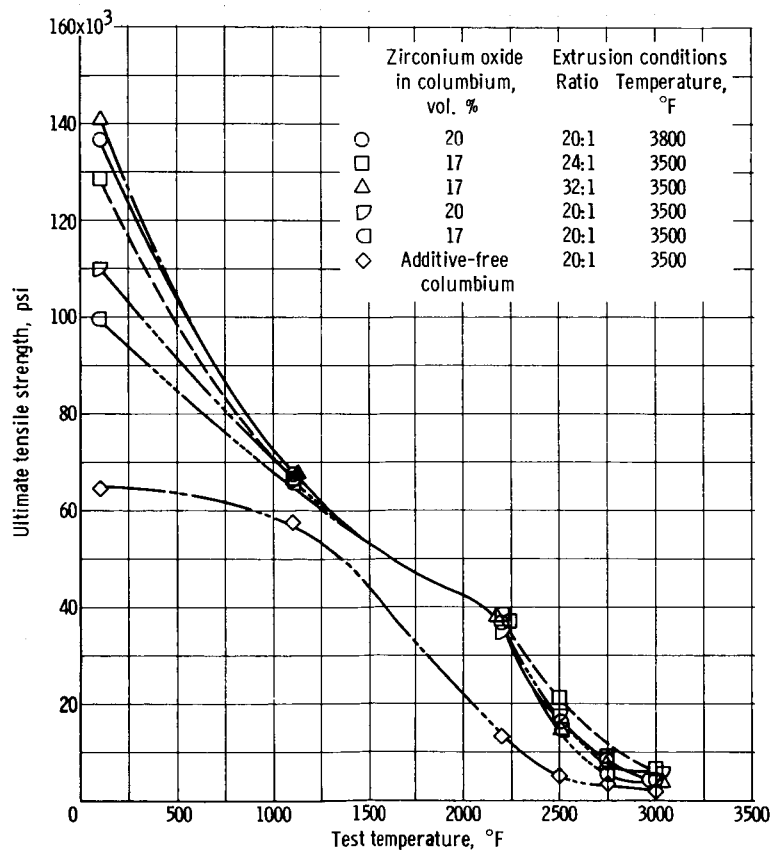


Figure 17. - Tensile strength of zirconium oxide - columbium composites at various temperatures.

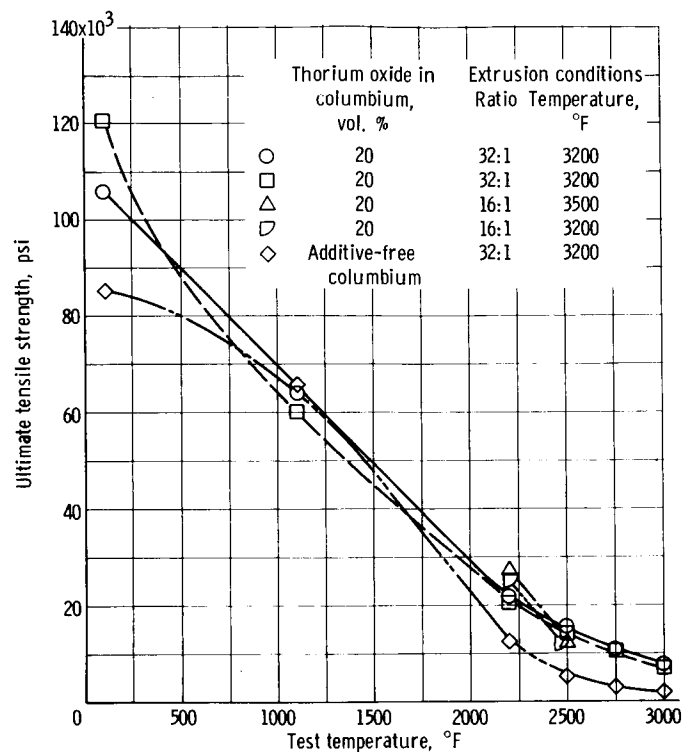


Figure 18. - Tensile strength of thorium oxide - columbium composites at various temperatures.

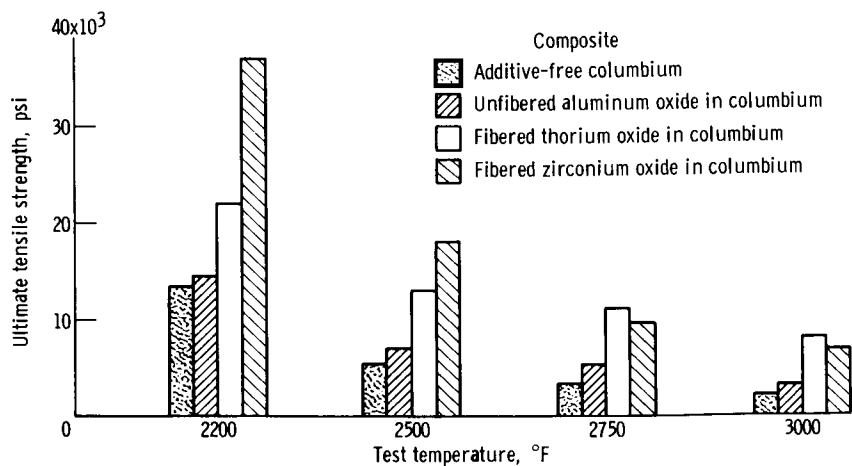


Figure 19. - Comparison of tensile strength of columbium composites containing fibred and unfibred oxides.

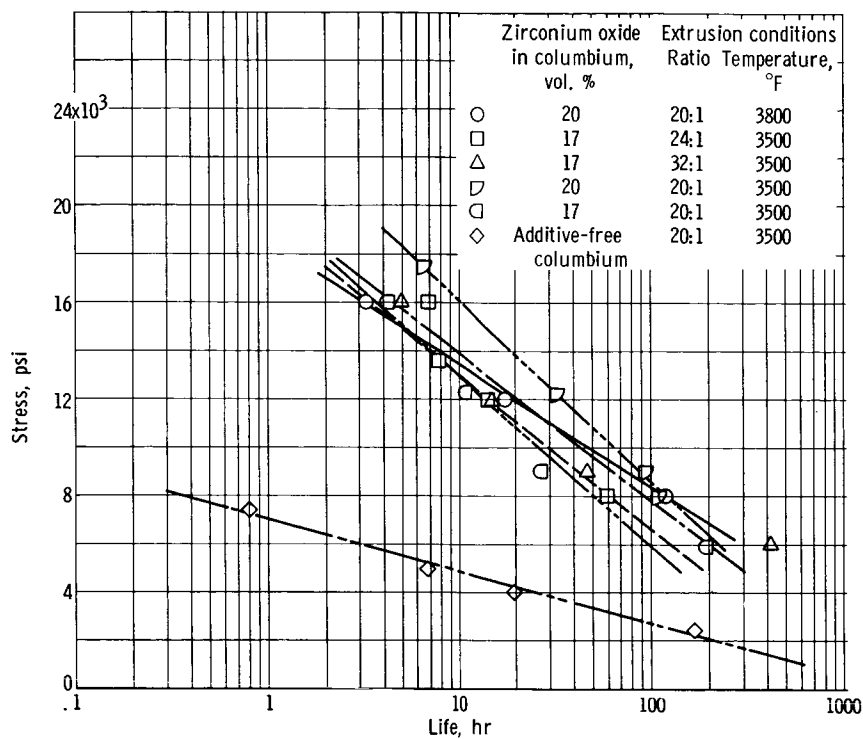


Figure 20. - Stress-rupture strength of zirconium oxide - columbium composites at 2200° F.

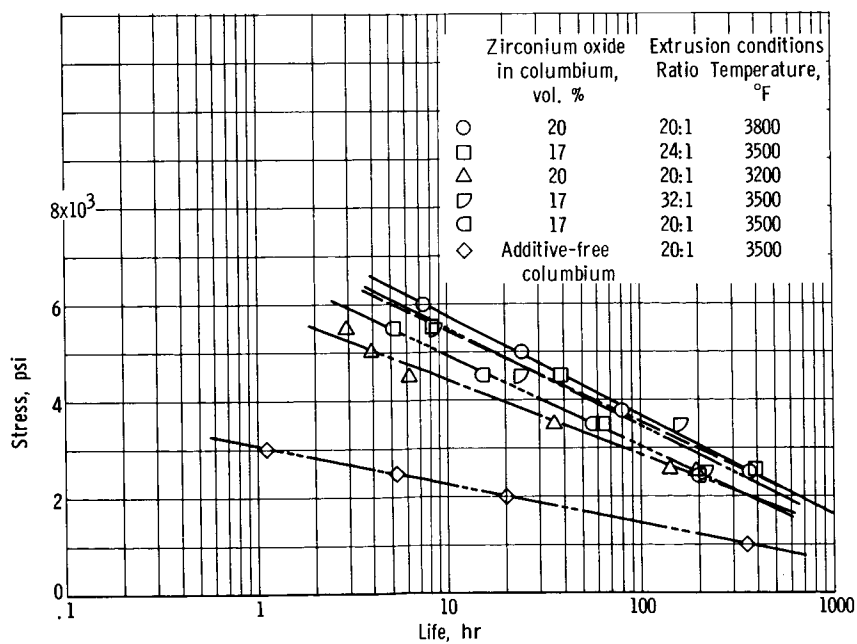


Figure 21. - Stress-rupture strength of zirconium oxide - columbium composites at 2500° F.

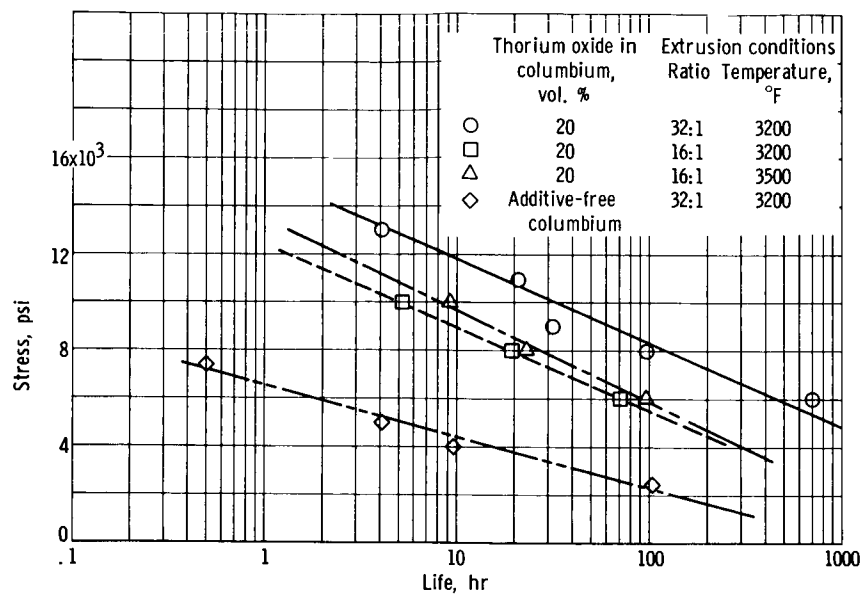


Figure 22. - Stress-rupture strength of thorium oxide - columbium composites at 2200° F.

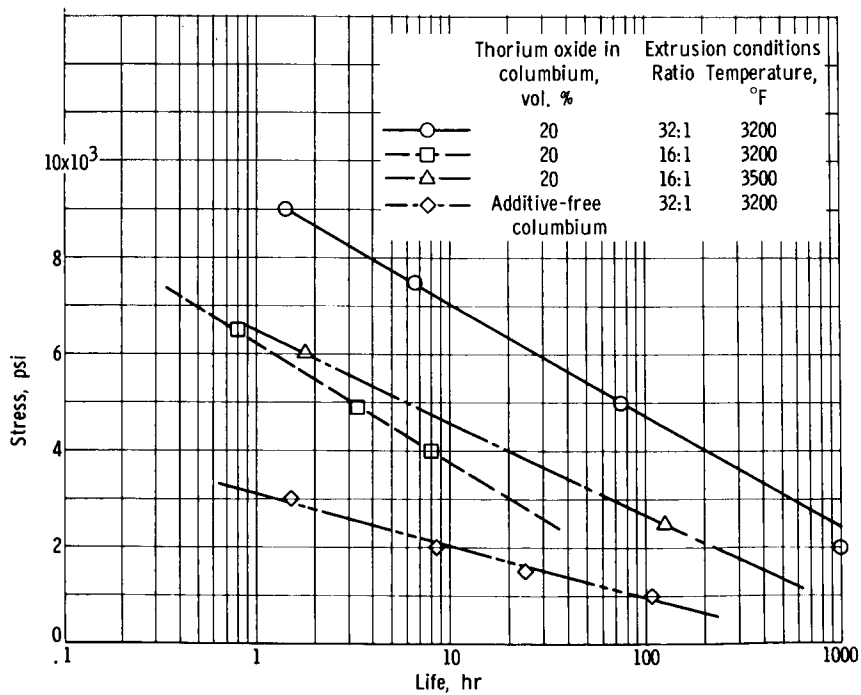
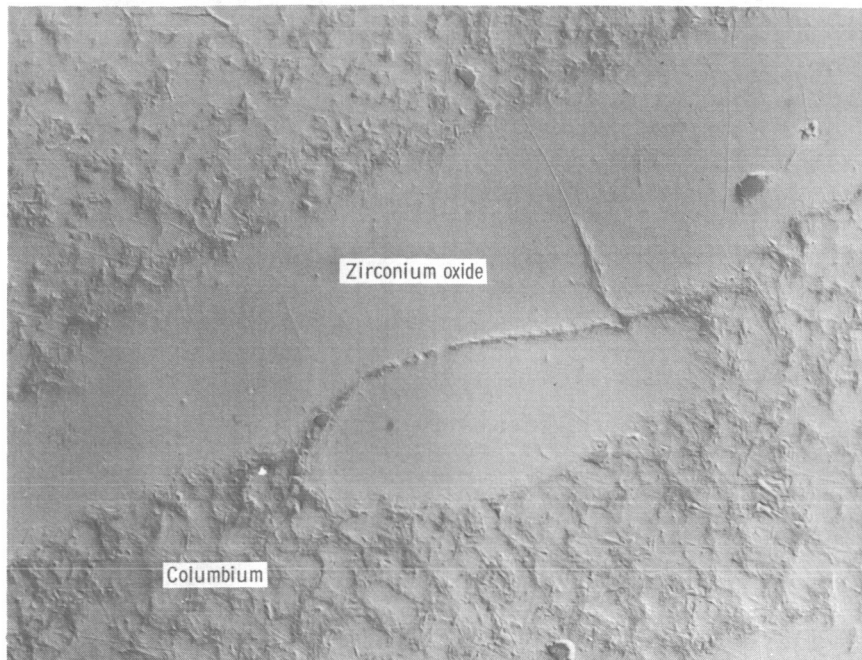
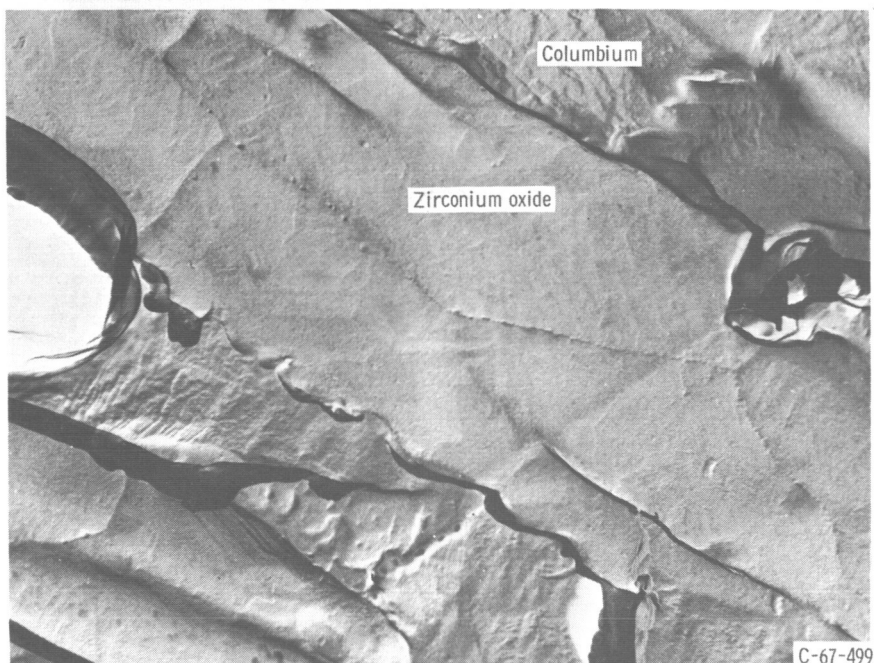


Figure 23. - Stress-rupture strength of thorium oxide - columbium composites at 2500° F.



(a) Unetched. X11 000.



(b) Etched. X17 000.

Figure 24. - Electron photomicrographs of zirconium oxide - columbium composites.
(Reduced 50 percent in printing.)

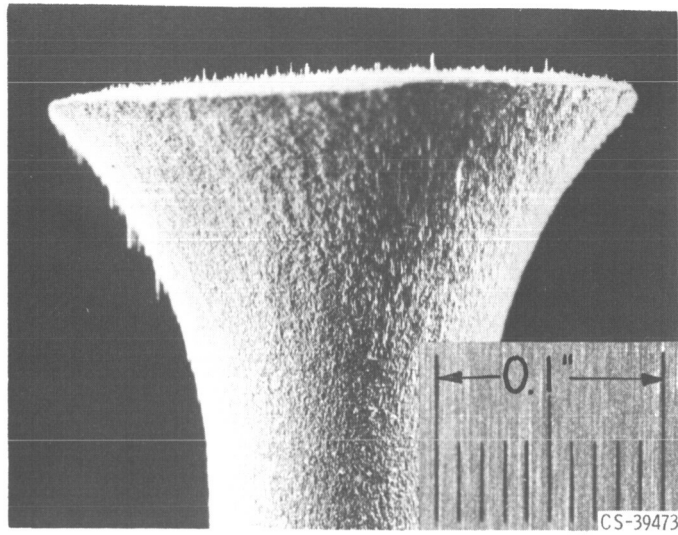


Figure 25. - Zirconium oxide fibers exposed after removal of columbium matrix by digestion.

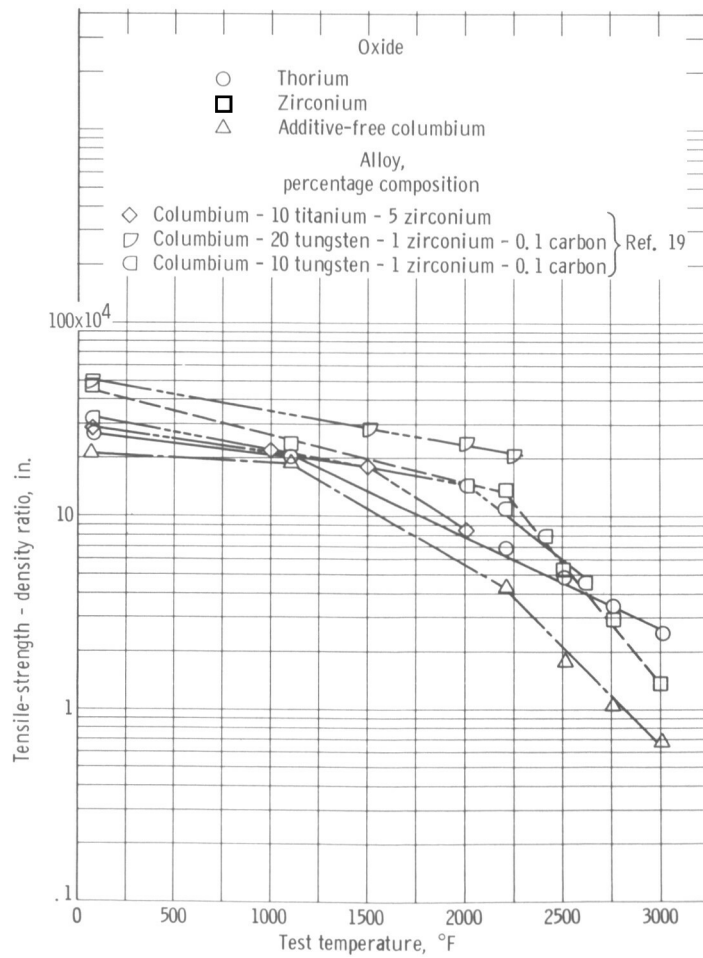


Figure 26. - Tensile-strength - density ratio of oxide-fiber - columbium composites and columbium alloys at various temperatures.

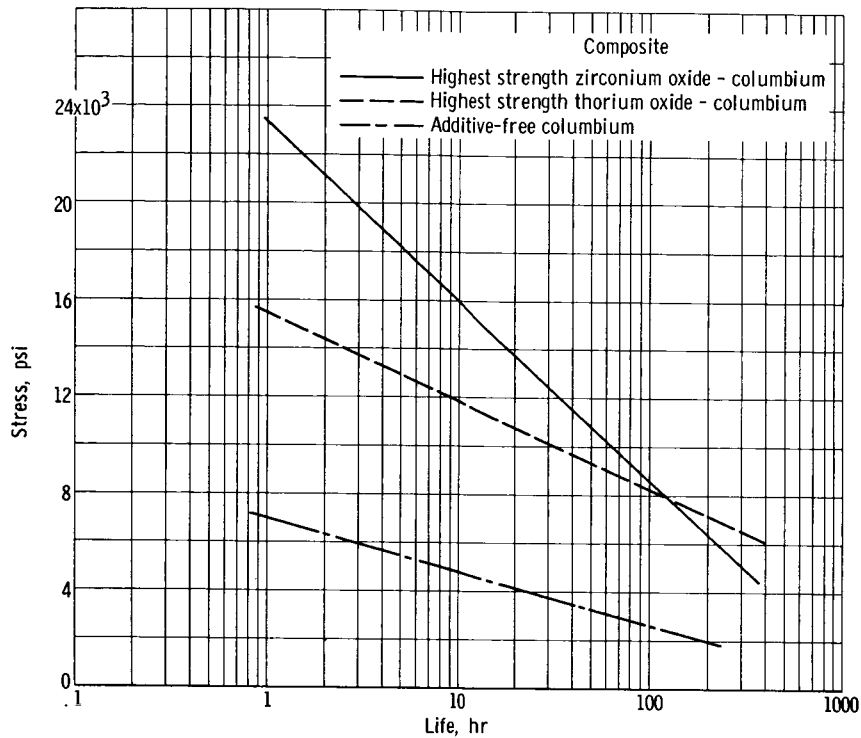


Figure 27. - Comparison of stress-rupture strength of additive-free columbium and zirconium oxide - columbium and thorium oxide - columbium composites at 2200° F.

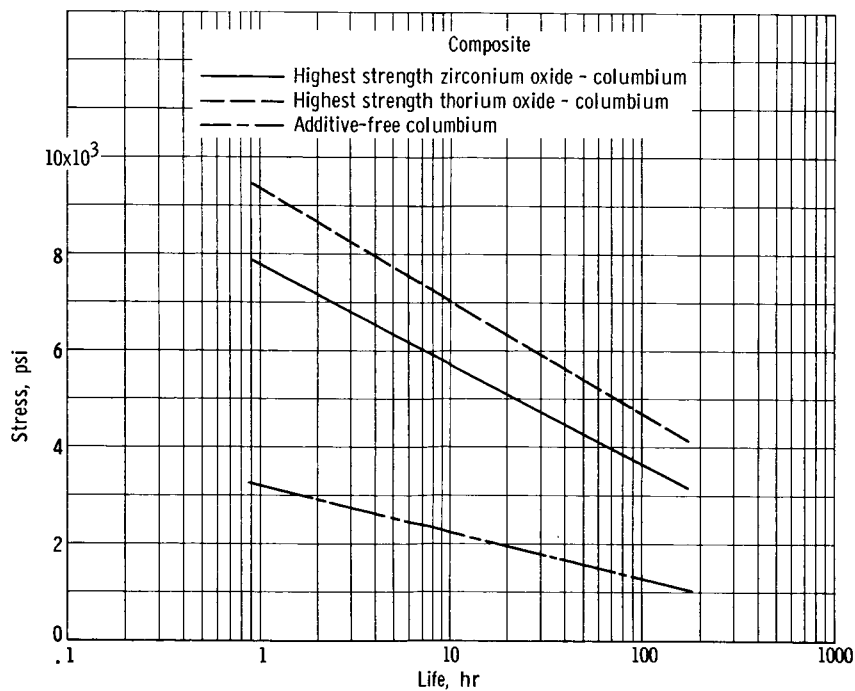


Figure 28. - Comparison of stress-rupture strength of additive-free columbium and zirconium oxide - columbium and thorium oxide - columbium composites at 2500° F.

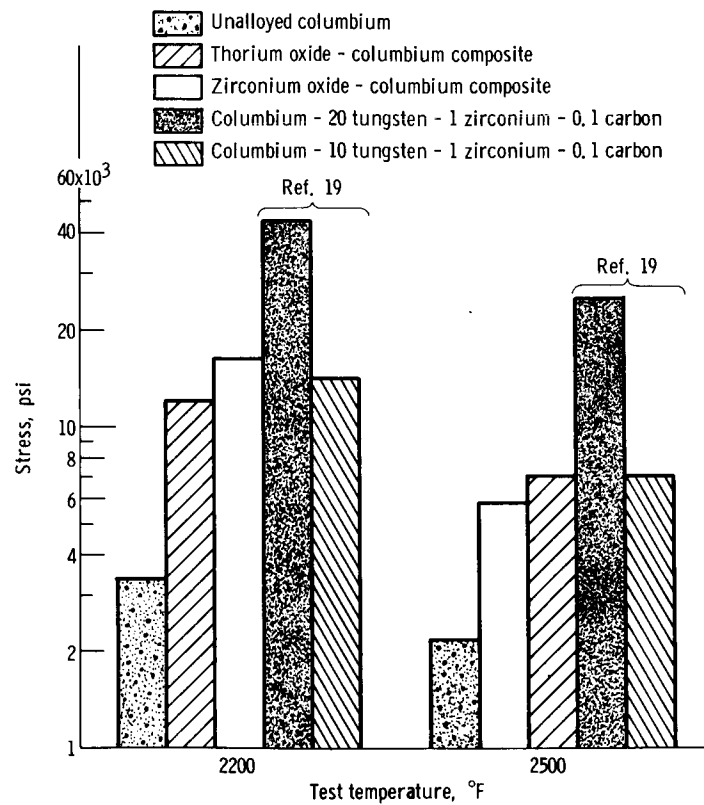


Figure 29. - Stress required to cause rupture of fibered-oxide - columbium composites and columbium alloys in 10 hours at 2200° and 2500° F.

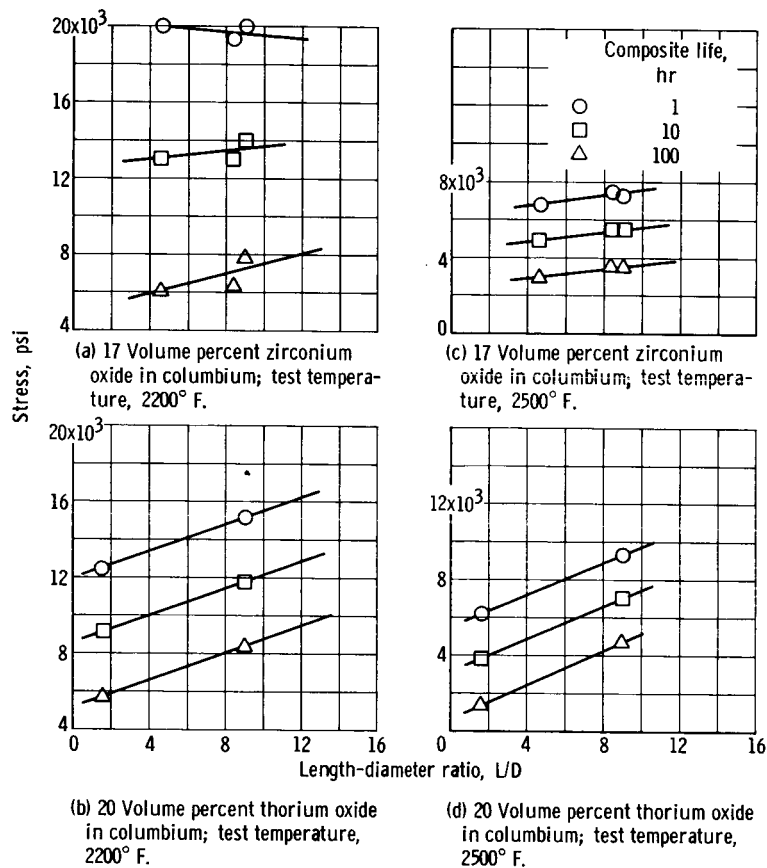


Figure 30. - Stress-rupture strength as function of fiber length-diameter ratio.